AD-A038 340 PURDUE UNIV LAFAYETTE IND F/G 20/12
THE EFFECTS OF SUBSTRATE COMPOSITION OF THICK FILM CIRCUIT RELI--ETC(U)
FEB 77 R W VEST N00019-76-C-0354
UNCLASSIFIED NL

| OF |
AD
A038340

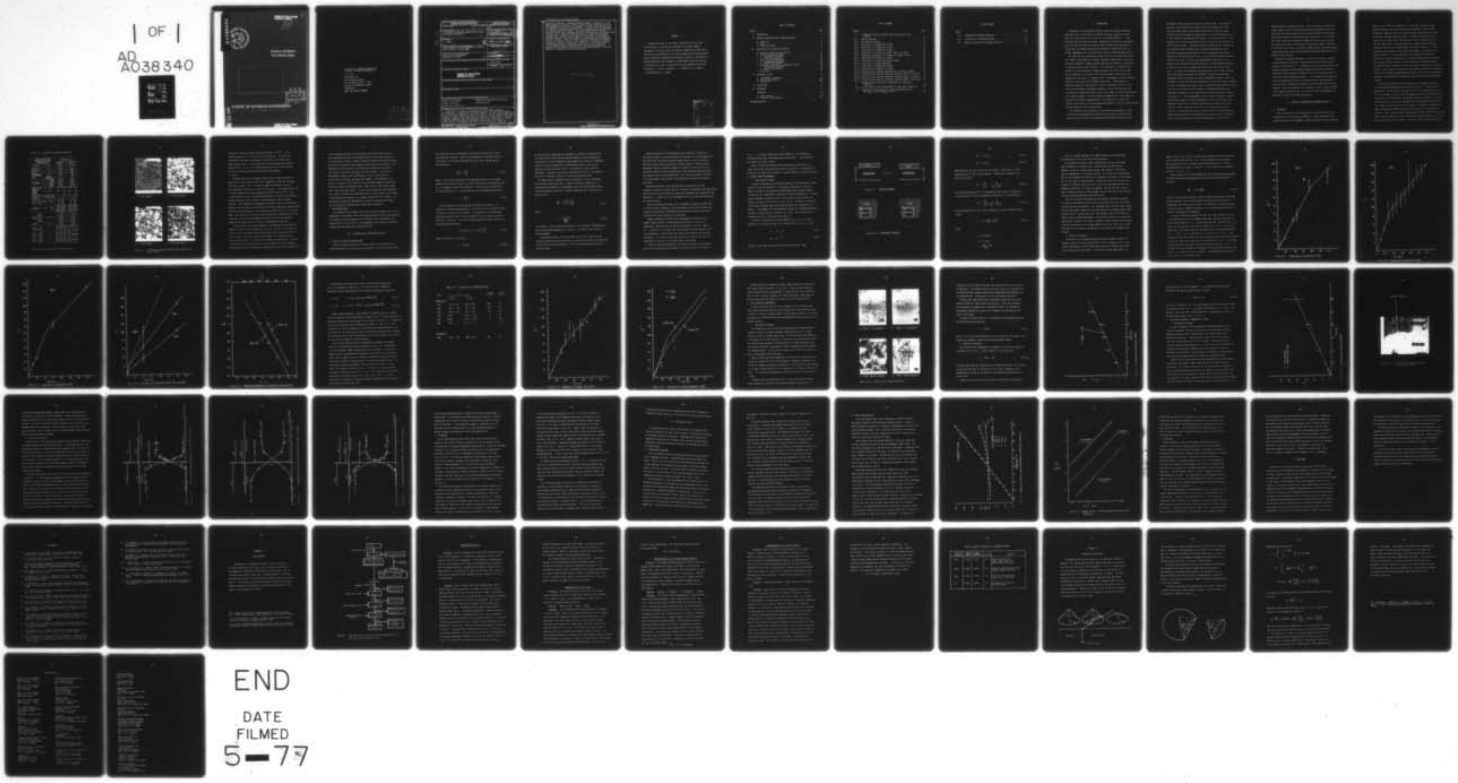

END

DATE
FILMED
5-77

FC

12

PURDUE UNIVERSITY

West Lafayette, Indiana

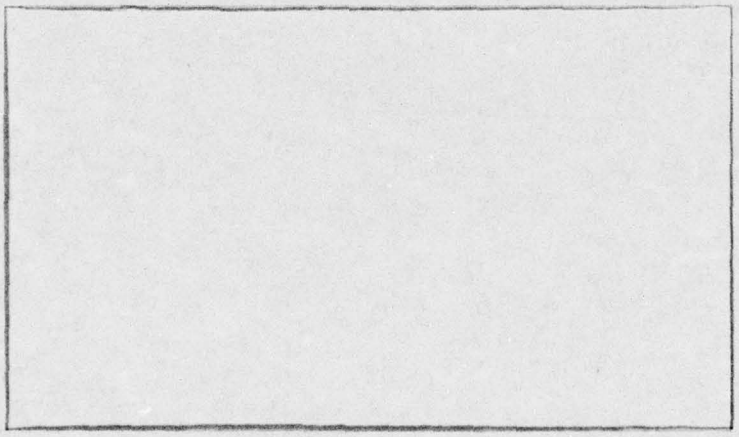

SCHOOL OF MATERIALS ENGINEERING

We forward + Contract

THE EFFECTS OF SUBSTRATE COMPOSITION ON THICK FILM CIRCUIT RELIABILITY

R. W. Vest

28 February 1977

Final Technical Report

For the period 2/1/76 - 1/31/77

Contract No. N00019-76-C-0354

Prepared for

NAVAL AIR SYSTEMS COMMAND

SECURITY CLASSIFICATION OF THIS PAGE *(When Data Entered)*

REPORT DOCUMENTATION PAGE

READ INSTRUCTIONS BEFORE COMPLETING FORM

1. REPORT NUMBER	2. GOVT ACCESSION NO.
3. RECIPIENT'S CATALOG NUMBER	
4. TITLE *(and Subtitle)* THE EFFECTS OF SUBSTRATE COMPOSITION ON THICK FILM CIRCUIT RELIABILITY	5. TYPE OF REPORT & PERIOD COVERED Final Report, 1 Feb 76 (2/1/76 to 1/31/77)
	6. PERFORMING ORG. REPORT NUMBER
7. AUTHOR(s) R. W. West	8. CONTRACT OR GRANT NUMBER(s) N00019-76-C-0354
9. PERFORMING ORGANIZATION NAME AND ADDRESS Purdue Research Foundation, Purdue University West Lafayette, Indiana 47907	10. PROGRAM ELEMENT, PROJECT, TASK AREA & WORK UNIT NUMBERS
11. CONTROLLING OFFICE NAME AND ADDRESS Naval Air Systems Command Washington, DC 20361	12. REPORT DATE 28 February 1977
	13. NUMBER OF PAGES 62
14. MONITORING AGENCY NAME & ADDRESS *(if different from Controlling Office)*	15. SECURITY CLASS. *(of this report)* Unclassified
	15a. DECLASSIFICATION/DOWNGRADING SCHEDULE N/A

16. DISTRIBUTION STATEMENT *(of this Report)*

APPROVED FOR PUBLIC RELEASE: DISTRIBUTION UNLIMITED

17. DISTRIBUTION STATEMENT *(of the abstract entered in Block 20, if different from Report)*

18. SUPPLEMENTARY NOTES

19. KEY WORDS *(Continue on reverse side if necessary and identify by block number)*

Thick film resistors
Ceramic substrates
Electrical resistivity
Temperature coefficient resistivity
Electronic glass

20. ABSTRACT *(Continue on reverse side if necessary and identify by block number)*

Studies of the rate of the dissolution of 96% Al_2O_3 substrates (AlSiMag 614) in a model glass (70% PbO, 20% B_2O_3, 10% SiO_2) were conducted as a function of temperature from 750 to 1000°C. The rate limiting steps were found to be phase boundary reaction rate control at short times and diffusion through a boundary layer under natural convection at longer times. The rate equations developed from the experimental data allow the prediction of the total quantity of substrate dissolved in the resistor glass under any

over

processing conditions. Standard processing (800°C, 10 minutes) for the model system will result in a fired resistor volume containing up to 20% of ingredients derived from the substrate. The rate of the dissolution of 99.5% Al_2O_3 substrates (AlSiMag 772) in the model glass was determined as a function of time at 800°C. The results were similar to those obtained for 96% Al_2O_3 substrates and were consistent with the proposed rate limiting steps. Studies of the distribution of substrate ingredients throughout the resistor glass at 800°C as a function of time produced results consistent with a step change in concentration at the substrate-resistor interface. Studies of the influence of substrate constituents dissolved in the glass on electrical properties of resistors uncovered a significant effect on temperature coefficient of resistance (TCR). A low TCR characteristic of reliable thick film resistors cannot be achieved with the model system unless an appreciable amount of substrate material is dissolved in the resistor glass.

FORWARD

Research described in this report constitutes the first year of effort under a contract with the Naval Air Systems Command, Department of the Navy, under the technical cognizance of James Willis. The research was conducted in the Turner Laboratory for Electroceramics, School of Materials Engineering and School of Electrical Engineering, Purdue University, West Lafayette, Indiana 47907, under the direction of Professor R. W. Vest. Contributing to the Project were Assistant Professor G. L. Fuller, and Messrs. J. M. Himelick, W. S. Machin, P. Palanisamy and R. L. Reed.

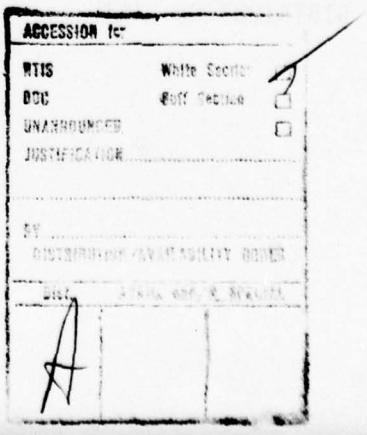

TABLE OF CONTENTS

Section		Page
I.	INTRODUCTION	1
II.	MATERIALS PREPARATION AND CHARACTERIZATION	3
	A. Substrates	3
	B. Glass	7
	C. Ruthenium Dioxide	8
III.	SUBSTRATE-GLASS INTERACTION KINETICS	8
	A. Review of Theory and Related Work	8
	B. Weight Change Measurements	12
	1. Experimental Procedure	12
	2. Results and Analysis	15
	C. Glass Analysis Measurements	26
	1. Experimental Procedure	26
	2. Results and Analysis	28
	D. Diffusion of Substrate Ingredients in Glass	30
	1. Experimental Procedure	30
	2. Results and Analysis	33
	E. Discussion	37
IV.	ELECTRICAL EFFECTS	39
	A. Experimental Procedures	39
	B. Results and Analysis	41
	C. Discussion	44
V.	FUTURE WORK	45
VI.	REFERENCES	47
	APPENDICES	49
	A. Glass Analysis	49
	B. Analysis of EDAX Results	57
	DISTRIBUTION LIST	

LIST OF FIGURES

Figure		Page
II.1	AlSiMag 614 Substrate Surfaces After Contact With Glass at 800°C	6
III.1	Resistor Geometry	13
III.2	Experimental Geometry	13
III.3	Dissolution of AlSiMag 614 at 750°C	17
III.4	Dissolution of AlSiMag 614 at 800°C	18
III.5	Dissolution of AlSiMag 614 at 850°C	19
III.6	Dissolution of AlSiMag 614 at 900°, 950°, and 1000°C	20
III.7	Temperature Dependence of AlSiMag 614 Dissolution Rate	21
III.8	Dissolution of AlSiMag 772 at 800°C	24
III.9	Dissolution of Alumina Substrates at 800°C	25
III.10	Single Crystal Alumina Substrates	27
III.11	Dissolution of AlSiMag 614 at 800°C	29
III.12	Dissolution of AlSiMag 614 at 800°C	31
III.13	Fracture Surface Showing Substrate-Glass Interface (6500X)	32
III.14	Diffusion Across Resistor-Substrate Interface (800°C, 4 minutes)	34
III.15	Diffusion Across Resistor-Substrate Interface (800°C, 8 minutes)	35
III.16	Diffusion Across Resistor-Substrate Interface (800°C, 10 minutes)	36
IV.1	Normalized Resistance Versus Temperature for RuO_2-Glass Composites	42
IV.2	Current Density-Field Relationships for RuO_2-Glass Composites	43
A.1	Flow-Sheet for the Separation and the Determinations of PbO, B_2O_3, SiO_2, and Al_2O_3 in Glass	50

LIST OF TABLES

Table		Page
II.1	Properties of Alumina Substrates	5
III.1	Dissolution of AlSiMag Substrates	24
A.1	Results of Analysis of Standard Chemicals	56

I. INTRODUCTION

"Substrate" is an unfortunate choice of words to describe the ceramic upon which thick film circuits are printed and fired, because this word implies an inert carrier when in fact it is an active material. It has been shown that the sheet resistance, temperature coefficient of resistance, and noise index of thick film resistors are affected by the substrate [1]. Studies have also demonstrated that the adhesion of conductives and its thermal degradation are a function of the choice of substrate material [2].

The print and fire processing of thick film circuits ensures that there will always be some degree of chemical interaction between the film and the substrate, because all common substrate materials are soluble to some degree in the glass used in thick film inks. This interaction is primarily responsible for the development of adhesion between the thick film resistor and the substrate. By virtue of the resistor-substrate interaction, the composition of the glass is changed, and as a consequence all of the physical properties of the glass will change to some extent. These changes in physical properties of the glass will result in modified kinetics for the various microstructure development processes in thick film resistors, and all electrical properties of the resistors are related to their microstructure. This research program is directed toward the determination of the effects of the major constituent, common additives, and impurities in alumina substrates on the kinetics of microstructure development, electrical characteristics and the adhesion of thick film resistors.

One influence of the substrate on microstructure development in thick film resistors was demonstrated during an earlier project at Purdue [13] involving X-ray diffraction line broadening experiments designed to study

the growth of RuO_2 conductive particles in the resistor. Test resistors prepared in the normal way by screen printing the formulation on 96% Al_2O_3 substrates showed a much slower growth rate of RuO_2 than samples prepared by mixing the RuO_2 and glass powders in the same proportions as in the formulation and heating this mixture in a platinum crucible. The presence of the substrate appeared to buffer the crystallite size after an initial rapid increase. X-ray phase analysis results did not indicate any new crystalline phases formed due to interactions between any of the ingredients (RuO_2-glass-substrate) for the time-temperature conditions employed in the ripening studies, but it was found that alumina was readily soluble in the glass. Contact angle measurements using glass with ten weight percent substrate material dissolved in it showed complete wetting to RuO_2, but the rate of spreading was much slower than for the normal glass. The glass would penetrate the RuO_2 particles at a slower rate and the driving forces responsible for the early stages of microstructure development would be displaced to higher temperatures; however, these temperatures are still well below the temperature range of the ripening studies. In order to determine the change in the viscosity and surface tension of the glass due to dissolution of the substrate, shrinkage measurements were conducted on compacts of glass powder with and without substrate material dissolved in it. The time dependence of the linear shrinkage of a compact consisting of spherical particles undergoing initial stage sintering by Newtonian viscous flow is directly proportional to time, and the proportionality constant contains the ratio of the surface tension to the viscosity. The surface tension to viscosity ratio for the glass with ten weight percent substrate dissolved was only one-fourth that of the normal glass, but this change was not nearly large enough to account for the

observed change in ripening kinetics. Since the results of neither the contact angle nor the viscosity-surface tension measurements using the glass with ten weight percent substrate material dissolved could explain the observed effect of substrate-resistor interactions, it was believed that these interactions changed the composition of the glass such that the solubility of RuO_2 in the glass was drastically reduced. Reduction in the solubility of RuO_2 in the glass further reduces the phase boundary reaction controlled solution-precipitation process and hence the rate of growth of RuO_2 particles.

Another role played by the glass in thick film resistors is that of a charge transport medium for a certain fraction of the total current carried by the resistor [3]. In addition to well sintered contacts in the conducting network, certain contacts between oxide particles contain a thin glass film and transport through this film is an important part of the overall charge transport mechanism. It is suspected that properties such as voltage coefficient of resistance and short time overload are very sensitively related to the number and the characteristics of these contacts. Electrical behavior of such contacts is very strongly related to the impurity content of the glass and hence would be expected to be sensitive to substrate-resistor interactions.

II. MATERIALS PREPARATION AND CHARACTERIZATION

A. SUBSTRATES

The two substrates used to develop base line data were 96% Al_2O_3 (AlSiMag 614) and 99.5% Al_2O_3 (AlSiMag 772). After discussions with technical personnel at 3M Company, 5,000 AlSiMag 614 substrates from the

same lot (S.O. 77318) were obtained. In order that all three related research programs could work with the same substrates, 3,000 of these AlSiMag 614 substrates were sent to RCA Princeton Laboratories and 1,000 to the Naval Research Laboratory (NRL). AlSiMag 772 substrates from a single lot (S.O. 88531) were also obtained; 1,500 of these were sent to RCA and 1,000 to NRL. The average physical property data published by 3M Company on these two substrate bodies are shown in Table II.1. These substrates were prepared by the ceramic tape process as disclosed in U.S. patent #2,966,719. The starting powder was prepared by adding small quantities of certain ingredients to a low soda alumina which is typically 99.7% Al_2O_3. The RCA research team will perform bulk chemical analyses on substrate bodies from the two single lots being utilized on this project. The NRL research team will characterize the surface composition of substrates from each lot by Auger spectroscopy and sputter profiles, and also determine preferred crystallographic orientation on the surfaces by X-ray diffraction analyses.

The size of Al_2O_3 grains in the substrates is an important parameter for understanding substrate-glass interaction kinetics. According to the manufacturer, surface crystals average 4.5 to 5 μm on AlSiMag 614 and 3 to 3.5 μm on AlSiMag 772, but no data are available on grain size distributions. Observations of the surfaces of AlSiMag 614 substrates from Lot S.O. 77318, as shown in Fig. II.1a, are in agreement with an average grain size of 4.5 - 5 μm. However, when the first layer of grains is removed by dissolution in glass a considerably different grain size and grain size distribution is observed. After 1 minute contact with the glass at 800°C, grains of 10 μm and larger begin to appear (Fig. II.1b) and after 3 minutes exposure (Fig. II.1c) the larger grains are very obvious. This grain size distribution does not

TABLE II.1 Properties of Alumina Substrates

Measurements shown are average values from unglazed test pieces. Production articles may vary slightly, depending on size, shape and method of manufacture.		COMPOSITION	
		ALSIMAG 614	ALSIMAG 772
PROPERTY	UNIT	96% Al_2O_3	99½% Al_2O_3
Water Absorption	%	0 Impervious	0 Impervious
Specific Gravity	— — —	3.70	3.89
Color	— — —	White	White
Safe Temperature at Continuous Heat	°C °F	1 550 2 822	1 600 3 002
Hardness	Mohs' Scale Rockwell 45 N	9 78	9 80
Thermal Expansion Linear Coefficient	Per °F: 70- 400°F	3.6×10^{-6}	3.3×10^{-6}
	Per °F: 70-1300°F	4.7×10^{-6}	4.2×10^{-6}
	Per °F: 70-1650°F	4.4×10^{-6}	4.6×10^{-6}
	Per °C: 25-300°C	6.4×10^{-6}	6.6×10^{-6}
	Per °C: 25-700°C	7.5×10^{-6}	7.4×10^{-6}
	Per °C: 25-900°C	7.9×10^{-6}	7.7×10^{-6}
Compressive Strength	Psi / Kg/cm²	375 000 / 26 360	380 000 / 26 720
Flexural Strength Sample Size: .025 thick .070 wide .500" span	Psi / Kg/cm²	60 000 / 4 220	70 000 / 4 920
Modules of Elasticity	PSI x 10^6 / KG/cm³ x 10^6	47 / 3.30	55 / 3.87
Shear Modulus	PSI x 10^6 / KG/cm² x 10^6	19 / 1.34	22 / 1.55
Poisson's Ratio	— — —	.22	.22
Thermal Conductivity 25°C	BTU in./hr. ft² °F / cal. cm./sec. cm² °C	244 / .084	255 / .088
Thermal Conductivity 300°C		119 / .041	130 / .045
Thermal Conductivity 500°C		75 / .026	81 / .028
Thermal Conductivity 800°C		58 / .020	61 / .021
Dielectric Strength 60 Hertz AC	volts per mil / Kilovolts per mm	AS FIRED SURFACES .010 thick 925 36.4 .025 thick 800 31.5 GROUND SURFACES .010 thick 900 35.4 .025 thick 700 27.6	AS FIRED SURFACES .010 thick 920 36.2 .025 thick 775 30.5 GROUND SURFACES .010 thick 900 35.4 .025 thick 725 28.5
Volume Resistivity 25°	Ohm-centimeters	$> 10^{14}$	$> 10^{14}$
Volume Resistivity 100°C		2.0×10^{13}	7.3×10^{13}
Volume Resistivity 300°C		1.1×10^{10}	8.6×10^{11}
Volume Resistivity 500°C		7.3×10^{7}	3.1×10^{9}
Volume Resistivity 700°C		3.5×10^{6}	1.5×10^{8}
Volume Resistivity 900°C		6.8×10^{5}	5.5×10^{6}
Te Value[b]	°C °F	840 1 544	1 000 1 832
		25°C / 300°C / 500°C	25°C / 100°C / 300°C
Dielectric Constant 1 MHz	— — —	9.3 / 9.5 / 10.8	10.5 / — / —
Dielectric Constant 10 GHz		9.2 / 9.3 / 9.4	9.8 / 9.9 / 10.1
Dielectric Constant 25 GHz		9.0 / 9.1 / 9.2	9.8 / — / —
Dissipation Factor 1 MHz	— — —	.0003 / .0027 / .0131	.0001 / — / —
Dissipation Factor 10 GHz		.0009 / .0010 / .0019	.00004 / .00005 / .00007
Dissipation Factor 25 GHz		.0009 / .0009 / .0019	.0001 / — / —
Loss Factor 1 MHz	— — —	.0028 / .0257 / .1415	.0011 / — / —
Loss Factor 10 GHz		.0082 / .0093 / .0179	.0004 / .0005 / .0007
Loss Factor 25 GHz		.0081 / .0082 / .0175	.001 / — / —

[b] Te value is the temperature at which a centimeter cube has a resistance of one megohm.

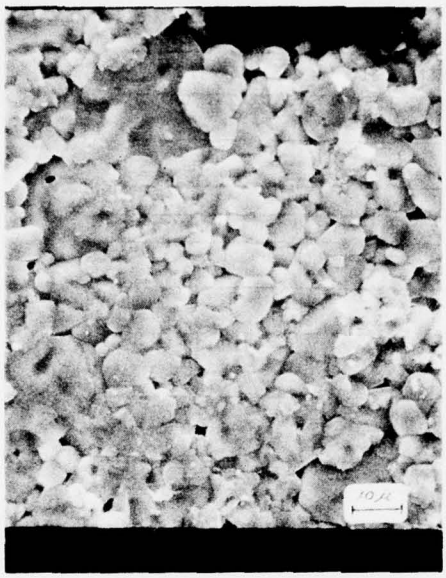

a. 0 min contact

b. 1 min contact

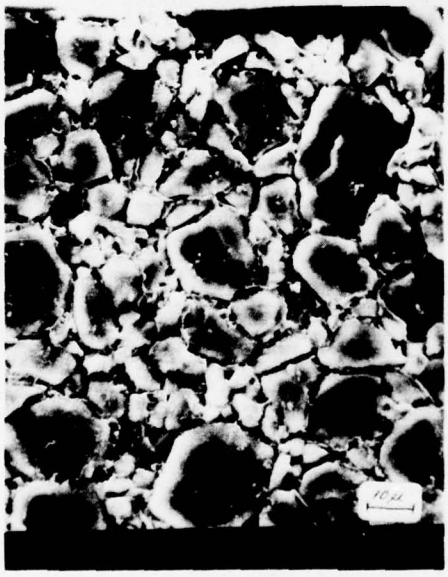

c. 3 min contact

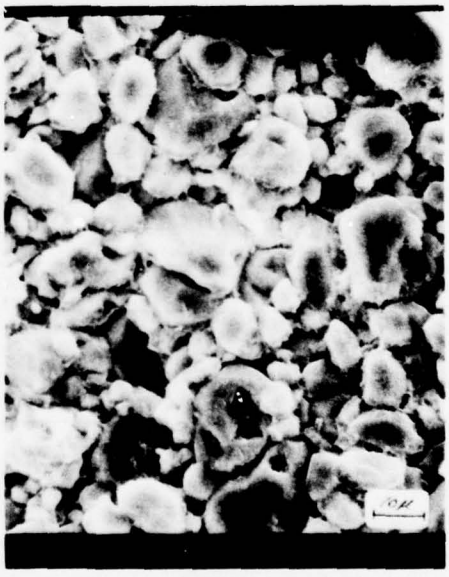

d. 720 min contact

Figure II.1 AlSiMag 614 Substrate Surfaces after Contact with Glass at 800°C

change with increasing contact time with the glass (see Fig. II.1d) indicating that this is the true bulk microstructure. The grain size distribution then must be considered in two parts, the surface layer having grains from 2 - 8 μm, and the bulk of the substrate having grains ranging from 2 - 15 μm. This layered microstructure is a direct result of the tape process by which the substrates were produced.

B. GLASS

The model glass used in previous studies [3] at Purdue on conduction mechanisms in thick film resistors had a composition of 63% PbO, 25% B_2O_3, 12% SiO_2 by weight. This is the glass composition specified in one of the fundamental patents [4] in thick film resistors. The thermal coefficient of linear expansion from room temperature to 300°C of 6.96×10^{-6}/°C [3] is very similar to that of the alumina substrates utilized and the ruthenium dioxide conductive, thus insuring a system relatively free of thermal stresses. High temperature measurements of surface tension by the modified dipping cylinder method, and viscosity by the sphere method were conducted [5], and the activation energy for the viscosity was found to by 81 ± 2 k/cal per mole. The sintering of spherical glass particles was studied [6] and it was found that the relationship between neck radius and time followed that predicted for Newtonian viscous flow as the predominant mechanism.

A consideration of the phase diagram for the $PbO-B_2O_3-SiO_2$ system [7,8] reveals that the 63-25-12 composition lies only a few wt % on the lead rich side of a two liquid phase region, and the later phase diagram work [8] on this system puts the composition at the boundary of a metastable region. For the present study it is necessary to change the composition of the glass by adding substrate ingredients (e.g. Al_2O_3 and MgO) and initial attempts to fabricate glasses by conventional techniques encountered some difficulties.

It was suspected that part of the problem arose from the fact that the base composition was near the metastable region of the phase diagram, so it was decided to choose a slightly different composition by moving directly away from the metastable region toward the PbO corner of the diagram. This composition, which was used in all model glass experiments described in this report, was 70% PbO, 20% B_2O_3, 10% SiO_2 by weight. The glass was fabricated by combining red lead (Pb_3O_4), a lead silicate glass frit (85 wt% PbO, 15 wt% SiO_2) and boric acid (H_3BO_3). The ingredients were mixed in a rolling jar for one hour, and the blended powder transferred to a platinum crucible and heated at 800 - 900°C until a single phase, bubble free, clear liquid was formed. In some cases the glass was used immediately (e.g. substrate weight loss experiments) while in other cases it was fritted in deionized water and ground in an agate vibratory mill to -325 mesh. An analytical procedure for determination of major constituents (PbO, B_2O_3, SiO_2 and Al_2O_3) was developed and is described in Appendix A.

C. RUTHENIUM DIOXIDE

The ruthenium dioxide powder used in this study was prepared by a careful dehydration of the hydrous oxide following procedures previously developed [3]. This powder had a BET surface area of 72 m^2/gram, which corresponds to an average particle size of 120 Å. The thermodynamic and electrical properties of RuO_2 have been extensively characterized [3].

III. SUBSTRATE-GLASS INTERACTION KINETICS

A. REVIEW OF THEORY AND RELATED WORK

There are several possible rate limiting steps for dissolution of an alumina substrate in a thick film resistor glass. At relatively short time

the dissolution rate is controlled by the chemical reation rate at the glass-substrate interface. When the concentration of substrate dissolved in the glass is well below the solubility limit, such a process may be described [9] by

$$\frac{dY}{dt} = K \frac{A_c}{A_o} \tag{III.1}$$

Where Y is the linear recession of the substrate surface, K is the phase-boundary reaction rate constant, A_c is the actual area of the substrate, and A_o is the geometric area of the substrate. If K and A_c are not functions of time, Equation III.1 is of zero order and can be integrated directly to

$$Y = K \frac{A_c}{A_o} t \tag{III.2}$$

As the concentration of solute near the interface increases it is necessary to remove substrate material in solution from the interface region in order for the reaction to continue. In the absence of flow-producing hydrostatic instabilities, the mass transport will be limited by molecular diffusion in the glass. This case has been analyzed by Cooper [10] and the following equation derived:

$$\pi^{\frac{1}{2}} \exp \alpha^2 \operatorname{erfc} \alpha = -\overline{V} \frac{C_i - C_m}{1 - \overline{V} C_i} \tag{III.3}$$

where the constant α is given by

$$\alpha = Y/2 \sqrt{D^* t} \tag{III.4}$$

C_i and C_m are the concentrations (expressed as fractions of the weight of the total melt) of the dissolved substrate material at the interface and in the melt, $\bar{V}$ is the incremental volume change in the glass per incremental volume of substrate added which is approximately equal to the ratio of substrate to glass densities, and D* is the effective binary diffusion coefficient. Equation III.4 predicts that there will be a $t^{\frac{1}{2}}$ time dependence for Y if molecular diffusion is the rate determining step.

At longer times, a boundary layer of thickness δ is built up between the interface and the bulk glass. Because of density, temperature, or surface tension gradients in the boundary layer, the region becomes hydrostatically unstable, resulting in natural convection and a recession rate given by [11],

$$\frac{dY}{dt} = \frac{D\,(C_i - C_m)}{\delta\,(1 - C_i\bar{V})} \qquad \text{(III.5)}$$

where

$$\delta = \frac{C_i - C_m}{\left(\frac{dC}{dx}\right)_i} \qquad \text{(III.6)}$$

and $(dC/dx)_i$ is the concentration gradient at the interface. Depending upon the relative time dependences of C_i and C_m, δ may show a wide variety of time dependences.

A considerable amount of work has been done with both single crystal and polycrystalline alumina dissolution in various glass melts under conditions of both free and forced convection. All of the mechanisms discussed above have been found.

Reed and Barrett [9, 12] investigated the dissolution of single and polycrystal alumina in calcium aluminum silicate melts of varying composition. They found that dissolution proceeds through chemical control, molecular diffusion control and free convection diffusion control. Rotating crystal experiments (forced convection) showed an increase in corrosion rate with increasing rotation velocity confirming the free convection mechanism after the boundary layer has been established. Very little difference in dissolution rates between single crystal and polycrystalline alumina was found at long times.

McCallum and Barrett [13] investigated the dissolution of single crystals of alumina in binary slags as a function of temperature and composition. The dissolution rate was found to be much more dependent upon temperature than composition. In addition it was concluded that the rate controlling mechanism was anion diffusion.

Studies by Cooper and Kingery [11] and Samaddar, Kingery and Cooper [14] of various ceramic compounds in calcium aluminum silicate melts showed that beyond very short times, dissolution was controlled initially by molecular diffusion and by free convection at long times.

Ryabov, Kiseleva and Kulikova [15] investigated the dissolution of alumina single crystals in molten potassium sulfate as a function of temperature, and found that the log of the dissolution rate was linear in 1/T. In addition it was found that the dissolution rate was dependent upon crystallographic orientation with the type of etch changing with changing orientation. The highest dissolution rate was on the basal plane and was approximately twice that on the other planes investigated.

Truhlarova [16] investigated the dissolution of single crystal alumina and silica and polycrystalline alumina in various glasses at a viscosity

of $\ln \eta = 2.5$ under conditions of free convection. No differences in dissolution rates were found between the various melts. The dissolution was found to be linear in time.

Safdar, Frischat and Hennicke [17] reported on the dissolution of single crystal and polycrystalline alumina in V_2O_5 melts. Dissolution was linear for all times with a decrease in slope at some time during the process.

B. WEIGHT CHANGE MEASUREMENTS

1. Experimental Procedure

In order to determine the dissolution kinetics of the substrates in the glass over long time periods ($t > 15$ minutes), experiments in which the change in weight of the substrate was determined after complete immersion in the glass were conducted as a function of time and temperature. To understand the geometry involved in thick film resistor firing, consider the process in going from Fig. III.1a, to Fig. III.1b. The glass in the thick film resistor dissolves away the printed surface of the substrate by an amount Y. The geometry of the experimental situation is somewhat different, as shown in going from Fig. III.2a to Fig. III.2b. Here the substrate is dissolved away on all surfaces by the amount Y.

Consider a substrate with initial dimensions $L_o \times L_o \times d_o$. After immersion in the glass for time t, its dimensions are $L_t \times L_t \times d_t$, with

$$L_o - L_t = 2Y \tag{III.7}$$

$$d_o - d_t = 2Y \tag{III.8}$$

where Y is the linear recession of the substrate surface. Now,

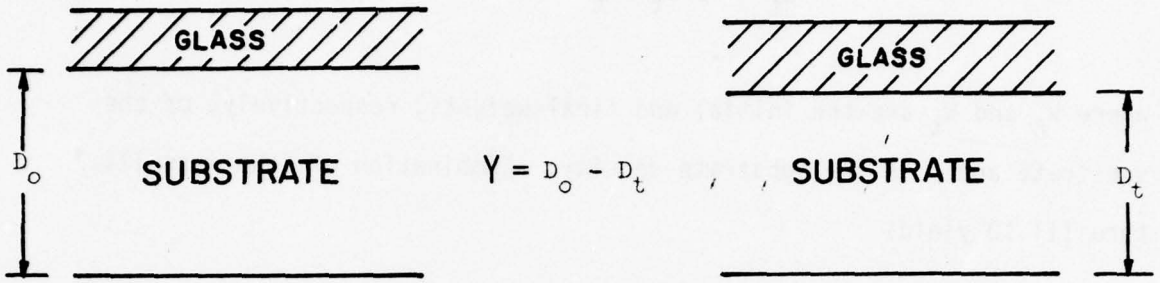

a. t = o b. t = t

Figure III.1 RESISTOR GEOMETRY

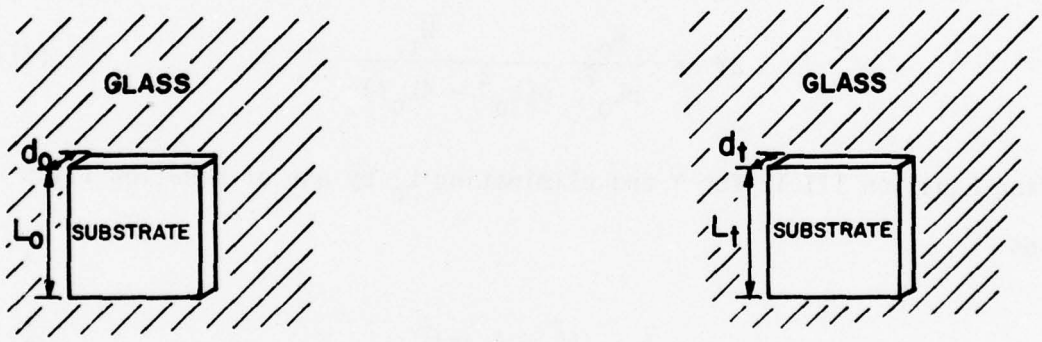

a. t = o b. t = t

Figure III.2 EXPERIMENTAL GEOMETRY

$$W_o = \rho L_o^2 d_o \qquad \text{(III.9)}$$

$$W_t = \rho L_t^2 d_t \qquad \text{(III.10)}$$

where W_o and W_t are the initial and final weights, respectively, of the substrate and ρ is the substrate density. Combination of Equations III.7 thru III.10 yields

$$2Y = \frac{W_o}{\rho L_o^2} - \frac{W_t}{\rho(L_o - 2Y)^2} \qquad \text{(III.11)}$$

Since the maximum value of Y is approximately 200 μm and L_o is typically 1 cm, the term in Y^2 can be neglected and Equation III.11 simplified to

$$2Y = \frac{W_o}{\rho L_o^2} - \frac{W_t}{\rho(L_o^2 - 4L_oY)} \qquad \text{(III.12)}$$

Solving Equation III.12 for Y and eliminating L_o by use of Equation III.9 yields

$$Y = \frac{b - (b^2 - 4ac)^{\frac{1}{2}}}{2a} \qquad \text{(III.13)}$$

where

$$a = 4\,(\rho d_o / W_o)^{\frac{1}{2}}$$

$$b = 1 + d_o a/2$$

$$c = \frac{d_o(W_o - W_t)}{2W_o}$$

Since d_o is known (0.64 mm), the linear recession can be calculated by measuring the initial and final substrate weights.

The procedure used was to clean a substrate by rinsing in deionized water followed by an acetone rinse. After drying, the substrate was weighed, secured in a platinum wire harness, and immersed in the molten glass at temperature in a platinum crucible. At the end of the time period, the chip was removed from the glass, air quenched, and placed in concentrated HCl to leach away the adhering glass. During this time, the chip was given 3 hours of ultrasonic agitation to aid in the glass decomposition and then allowed to stand until all glass was removed. The chip was then rinsed in water followed by acetone, dried, weighed, and the recession of the substrate surface calculated according to Equation III.13.

Two sets of control experiments were conducted to determine the degree of attack of the substrate alone by HCl and to assure that all of the glass was dissolved by the procedure. Four substrates which had never been exposed to glass were taken through the acid leach process; the average weight change was less than 0.1 mg which was within the accuracy limit of the analytical balance used for these measurements. For the second control, six substrates were dipped in glass for less than 10 seconds at 800°C and then taken through the acid leach process; the average weight loss was less than 0.3 mg indicating that all of the glass was removed to the accuracy that weighings could be made.

2. Results and Analysis

Experiments using AlSiMag 614 substrates were performed at 800°C for exposure times of 30 and 60 minutes and in 1 hour increments up to 12 hours. Similar measurements, but with fewer datum points per isotherm, were taken at 750, 850, 900, 950 and 1000°C. The results of these measurements are

shown in Figs. III.3 - III.6. At least three samples were run at each time and the vertical bars on Figs. III.3 - III.6 represent the spread among these samples with the solid point indicating the mean value. The best representation for all data is linear in t at all times, with a change in slope at $t = t_c$ and $Y = Y_c$.

Several sources [9,13,14,17] suggest that the time-temperature dependence of dissolution may be represented empirically by an Arrhenius equation of the form

$$\frac{dY}{dt} = A \exp\left[\frac{-E}{RT}\right] \qquad \text{(III.14)}$$

where E is the activation energy of the rate controlling process. Since many factors involved in the various dissolution mechanisms are functions of temperature, one should be very careful in assigning this activation energy to any one process. However, Equation III.14 is a good empirical representation of the temperature dependence.

In order to generate an equation of this form, least squares fits were first calculated for all line segments where there was sufficient data; i.e. at 750, 800 and 850°C for $t < t_c$, and at 800, 850, 900, and 950°C for $t > t_c$. These fits are shown as solid lines on Figures III.3 - III.6. The natural logarithim of the linear recession rate (dY/dt) was then plotted separately for $t < t_c$ and $t > t_c$ as a function of $1/T$ as shown in Fig. III.7. Least squares fits for these points were then calculated and the results extrapolated to find the slopes which could not be calculated earlier. For $t < t_c$ at 900, 950 and 1000°C the lines were fitted to go through the origin. For $t > t_c$ at 1000°C the line was made to go through the one datum point available, and for $t > t_c$ at 750°C the fit was estimated. The extrapolations are shown in Figs. III.3 - III.7 as dashed lines.

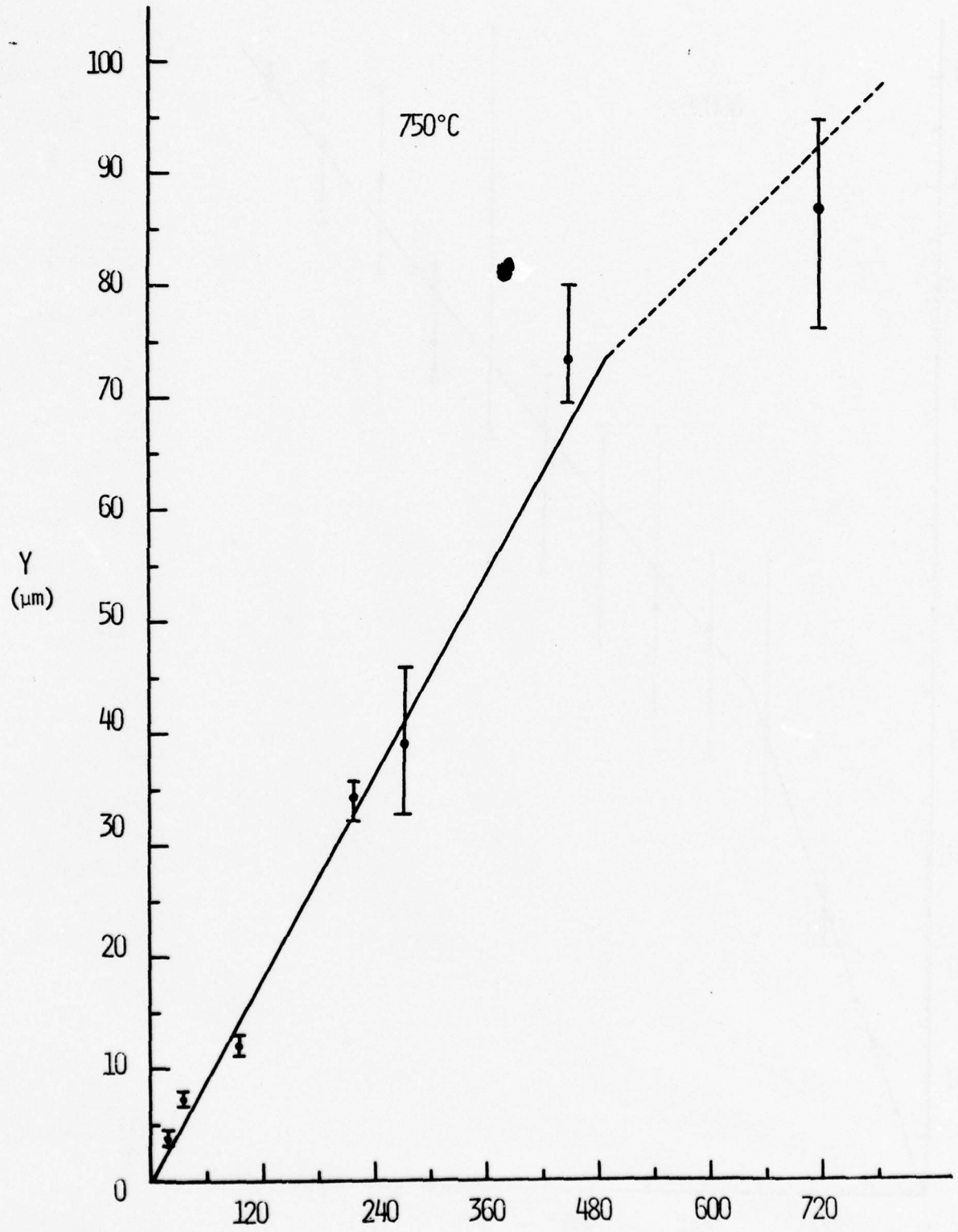

Figure III.3 DISSOLUTION OF ALSIMAG 614 AT 750°C

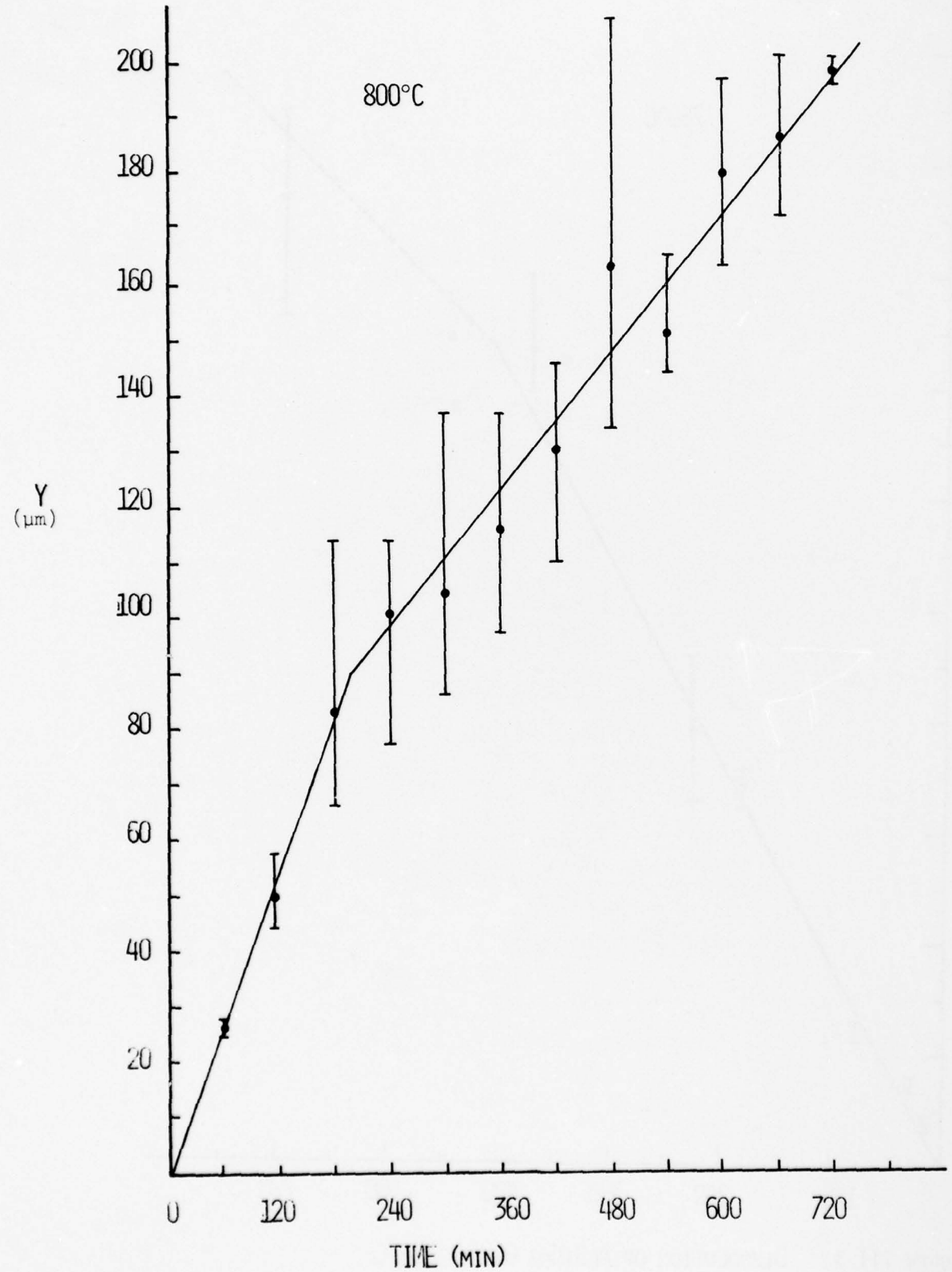

Figure III.4 DISSOLUTION OF ALSIMAG 614 AT 800°C

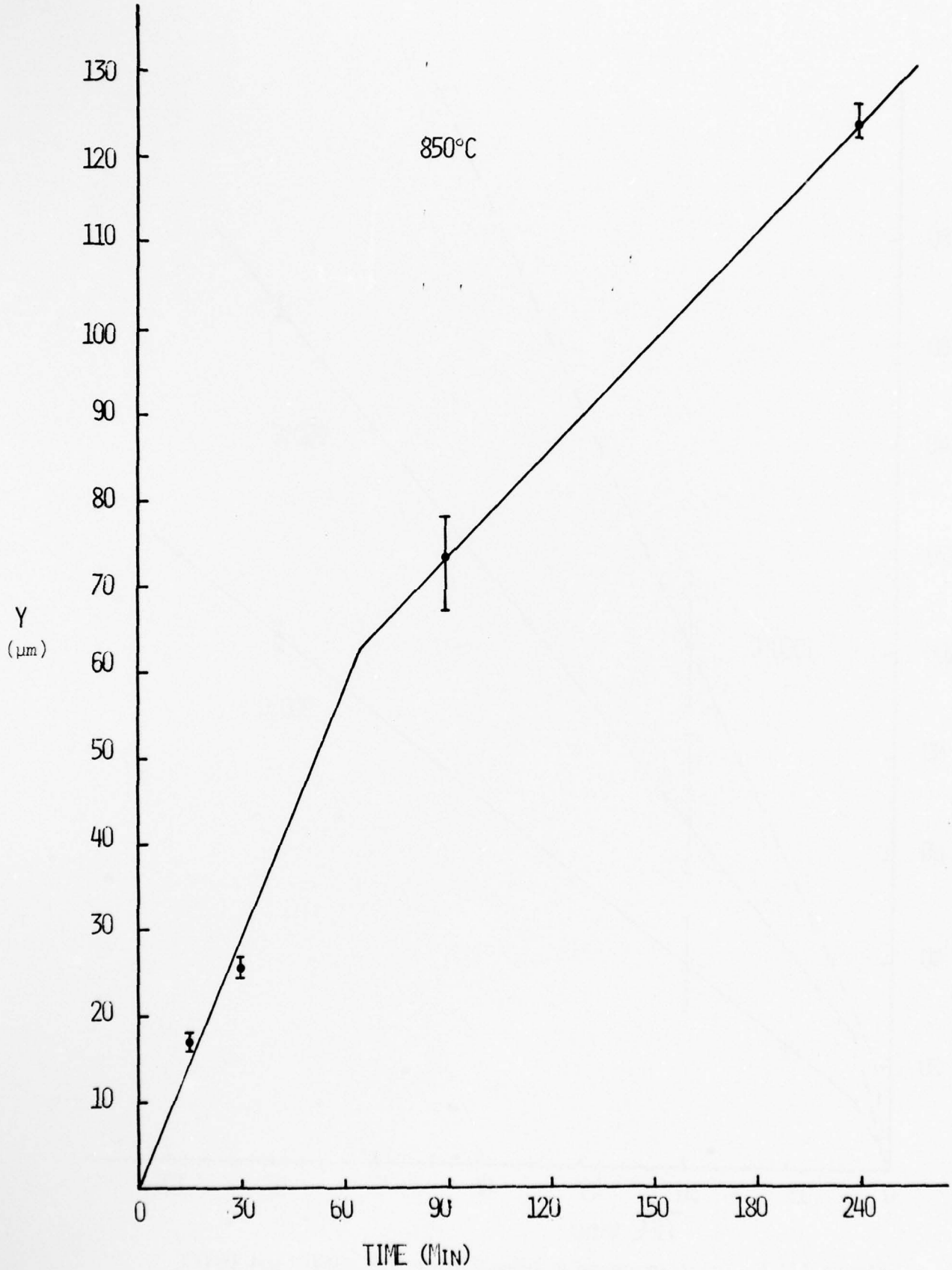

Figure III.5 DISSOLUTION OF ALSIMAG 614 AT 850°C

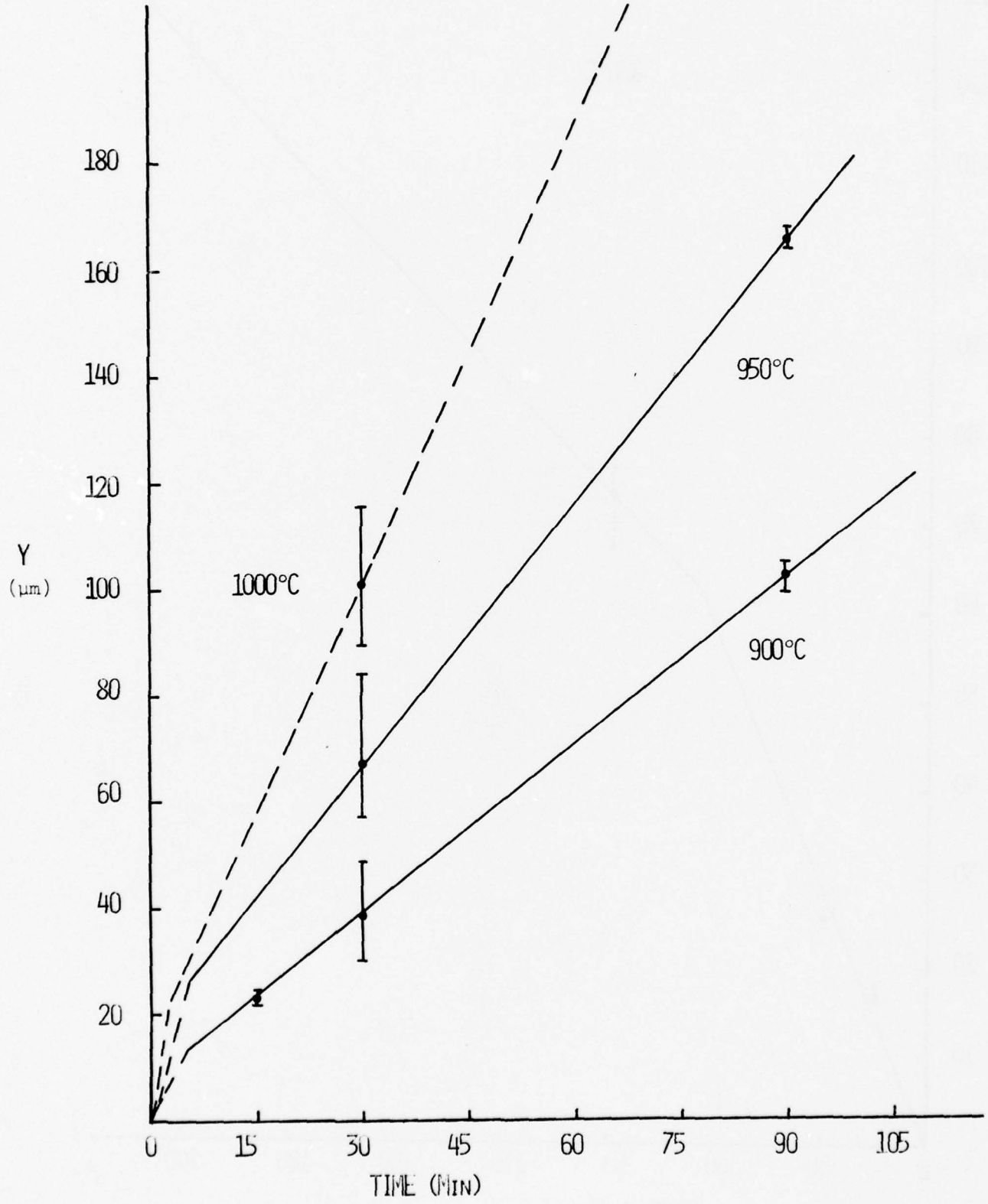

Figure III.6 DISSOLUTION OF ALSIMAG 614 AT 900°, 950° AND 1000°C

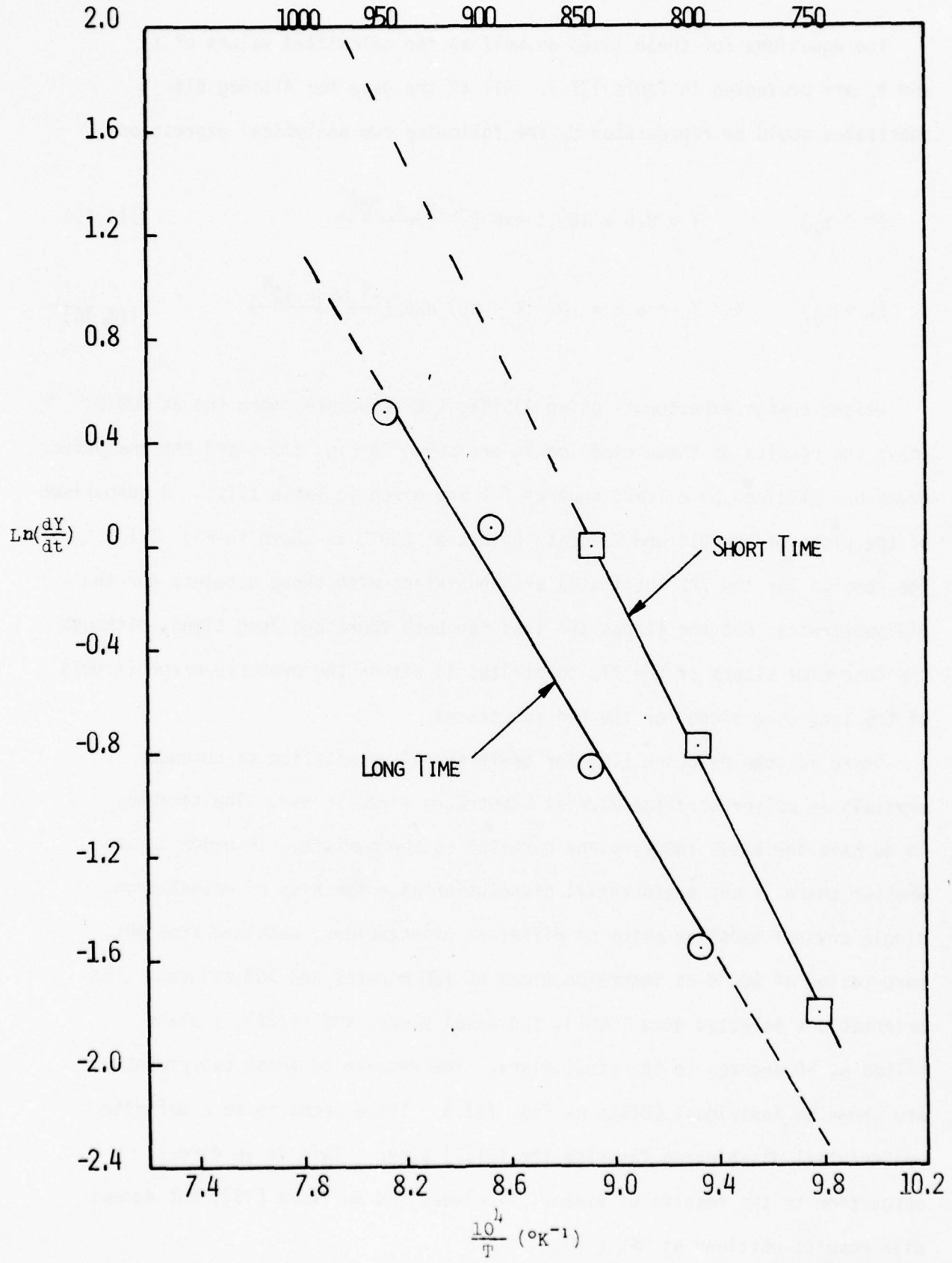

Figure III.7 TEMPERATURE DEPENDENCE OF ALSIMAG 614 DISSOLUTION RATE

The equations for these lines as well as the calculated values of t_c and Y_c are presented in Table III.1. All of the data for AlSiMag 614 substrates could be represented by the following two analytical expressions:

$$(t < t_c) \qquad Y = 8.6 \times 10^7 \, t \exp\left[\frac{-2.06 \times 10^4}{T}\right] \qquad \text{(III.15)}$$

$$(t > t_c) \qquad Y = Y_c + 6.5 \times 10^6 \, (t - t_c) \exp\left[\frac{-1.85 \times 10^4}{T}\right] \qquad \text{(III.16)}$$

Weight change experiments using AlSiMag 772 substrates were run at 800°C only; the results of these experiments are shown in Fig. III.8 and the analytical equations obtained by a least squares fit are given in Table III.1. A comparison of the plots of the 614 and 772 data points at 800°C is shown in Fig. III.9. The results for the 772 substrates are consistent with those obtained for the 614 substrates; but the slopes are less for both short and long times, although the long time slopes of the 772 substrates is within the probable error (±.052) of the long time slope for the 614 substrates.

There is some evidence [18] for preferential orientation of corundum crystals in polycrystalline alumina substrates fired in air. The tendency is to have the basal (0001) plane parallel to the surface. In order to see whether there is any preferential dissolution as a function of orientation, single crystal sapphire chips of different orientations, obtained from NRL, were tested at 800°C at immersion times of 120 minutes and 300 minutes. The orientations selected were (0001), the basal plane, and $(11\bar{2}3)$, a plane tilted at 60 degrees to the basal plane. The results of these experiments are shown as individual points on Fig. III.9. There seems to be a definite preferential dissolution favoring the $(11\bar{2}3)$ plane. This is in direct opposition to the results of Ryabov, Kiseleva, and Kulikova [15], but agrees with results obtained at NRL [19].

TABLE III.1 Dissolution of AlSiMag Substrates

T°C	Y		t_c(min)	Y_c(μm)
	$t < t_c$	$t > t_c$		
AlSiMag 614				
750	.14 t + 2.8	.091 t + 46	528	71
800	.44 t + .16	.21 t + 43	187	82
850	.87 t + 1.11	.41 t + 36	76	66
900	1.99 t	1.05 t + 7.5	8	16
950	4.08 t	1.6 t + 17.3	7	28
1000	7.92 t	3.2 t + 5	1	8.4
AlSiMag 772				
800	.35 t - .89	.185 t + 42	234	81

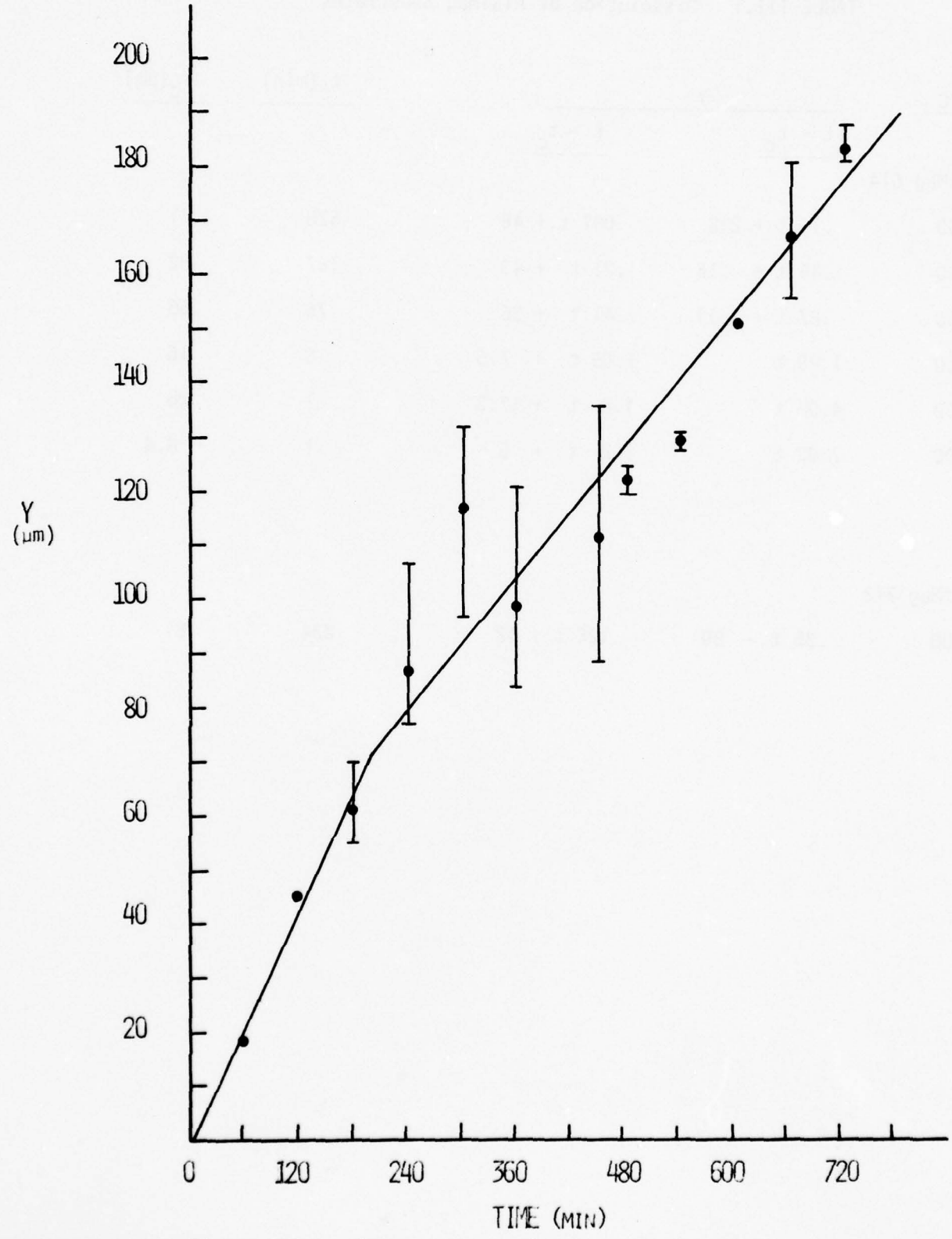

Figure III.8 DISSOLUTION OF ALSIMAG 772 AT 800°C

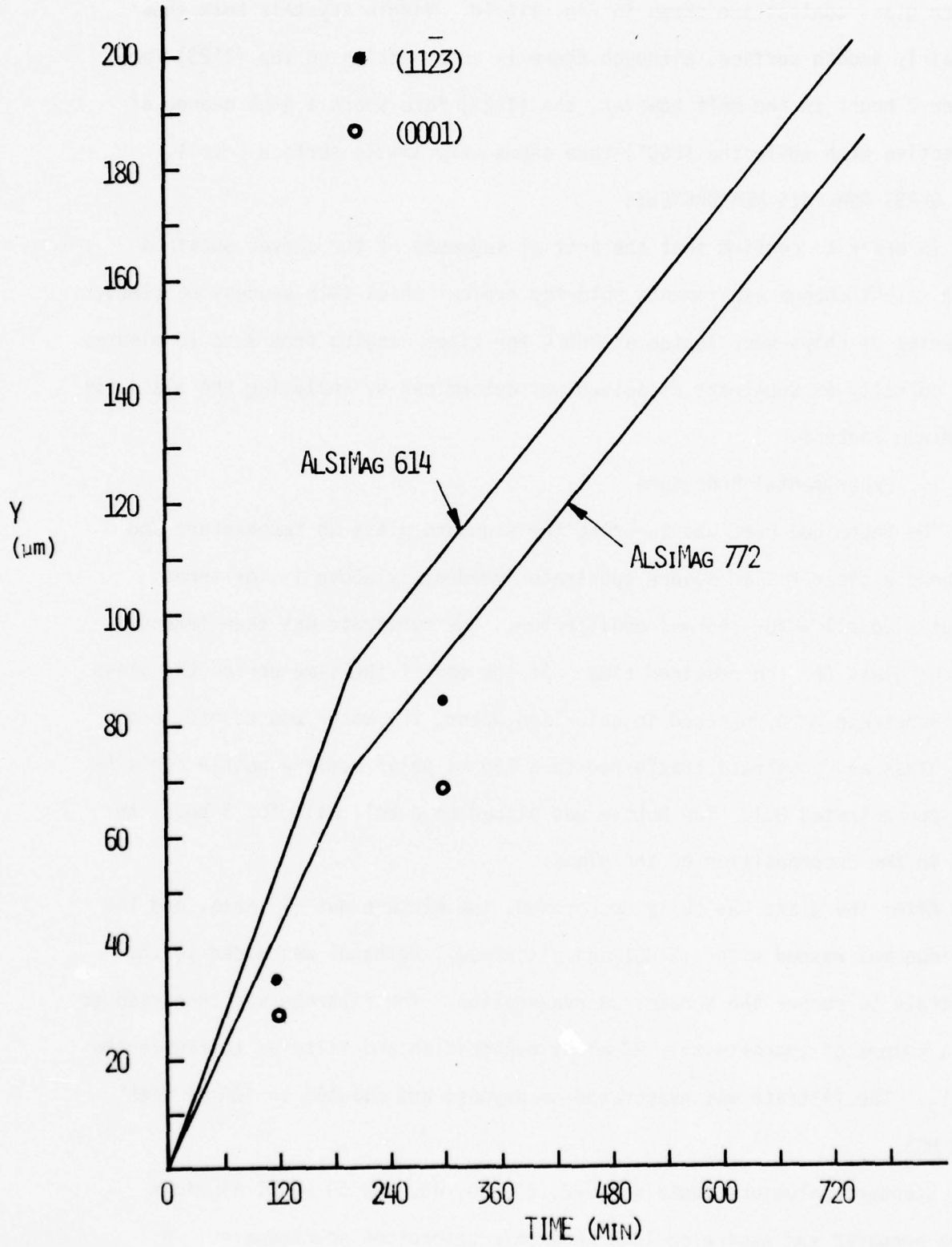

Figure III.9 DISSOLUTION OF ALUMINA SUBSTRATES AT 800°C

Scanning electron micrographs of these single crystals both before and after glass contact are shown in Fig. III.10. Virgin crystals both show a fairly smooth surface, although there is some pitting on the $(11\bar{2}3)$ face. After 2 hours in the melt however, the $(11\bar{2}3)$ face shows a high degree of selective etch while the (0001) face shows very little surface detail.

C. GLASS ANALYSIS MEASUREMENTS

In order to confirm that the initial segments of the curves obtained from weight change experiments hold for typical thick film processing times, a series of chips were tested at 800°C for times ranging from 3 to 15 minutes. The quantity of substrate dissolved was determined by analyzing the glass for aluminum content.

1. Experimental Procedure

The technique used was to bring the standard glass to temperature and suspend a clean 2.5 cm square substrate immediately above it for three minutes to allow for thermal equilibrium. The substrate was then immersed in the glass for the required time. At the end of the time period the glass and substrate were quenched in deionized water, the water poured off, and the glass and substrate trasferred to a 250 ml polypropylene bottle containing concentrated HCl. The bottle was placed on a roll mill for 3 hours to aid in the decomposition of the glass.

After the glass was fully decomposed, the mixture was filtered, and the residue was washed with .1N HCl and discarded. Methanol was added to the filtrate to remove the borates on evaporation. The filtrate was then reduced to a volume of approximately 20 ml by evaporation and filtered to remove the $PbCl_2$. The filtrate was evaporated to dryness and diluted to 100 ml with .1N HCl.

Standard solutions containing 10, 20, 30, 40, and 50 μg/ml aluminum were prepared and aspirated into an atomic absorption spectrometer. A

a. $(11\bar{2}3)$ 0 min exposure

b. (0001) 0 min exposure

c. $(11\bar{2}3)$ 300 min exposure

d. (0001) 300 min exposure

Figure III.10 Single Crystal Alumina Substrates

standard curve was prepared from these data showing μg/ml Al as a function of absorbance. Experimental samples were then diluted 5:1, aspirated into the unit, and their aluminum concentrations determined from absorbance and the standard curve. The relative error in this analysis was 10%.

A blank glass sample which had no substrate contact was also run and found to contain 0.1 μg/ml Al per gram of glass. Since this correction was significant in comparison to experimental values, the raw data was corrected by subtracting a factor of 0.1W where W was the weight of the glass in the sample.

In order to convert μg/ml to Y, the recession of the substrate surface, the following equation was used.

$$Y = .206\ Z \qquad \text{(III.17)}$$

where Z is the corrected concentration of Al in μg/ml and the constant .206 contains all geometric, density and molecular weight factors.

2. Results and Analysis

The results of this experiment were plotted as a function of time and are shown in Fig. III.11. A least squares fit to the data gave

$$Y = .441t + 1.04 \qquad \text{(III.18)}$$

It may be noted that this line does not go through the origin. This behavior may be real, but there is the possibility of a small systematic error, perhaps due to milling of the surface of the substrate during the time on the ball mill.

Combining the data for this experiment with the data for AlSiMag 614

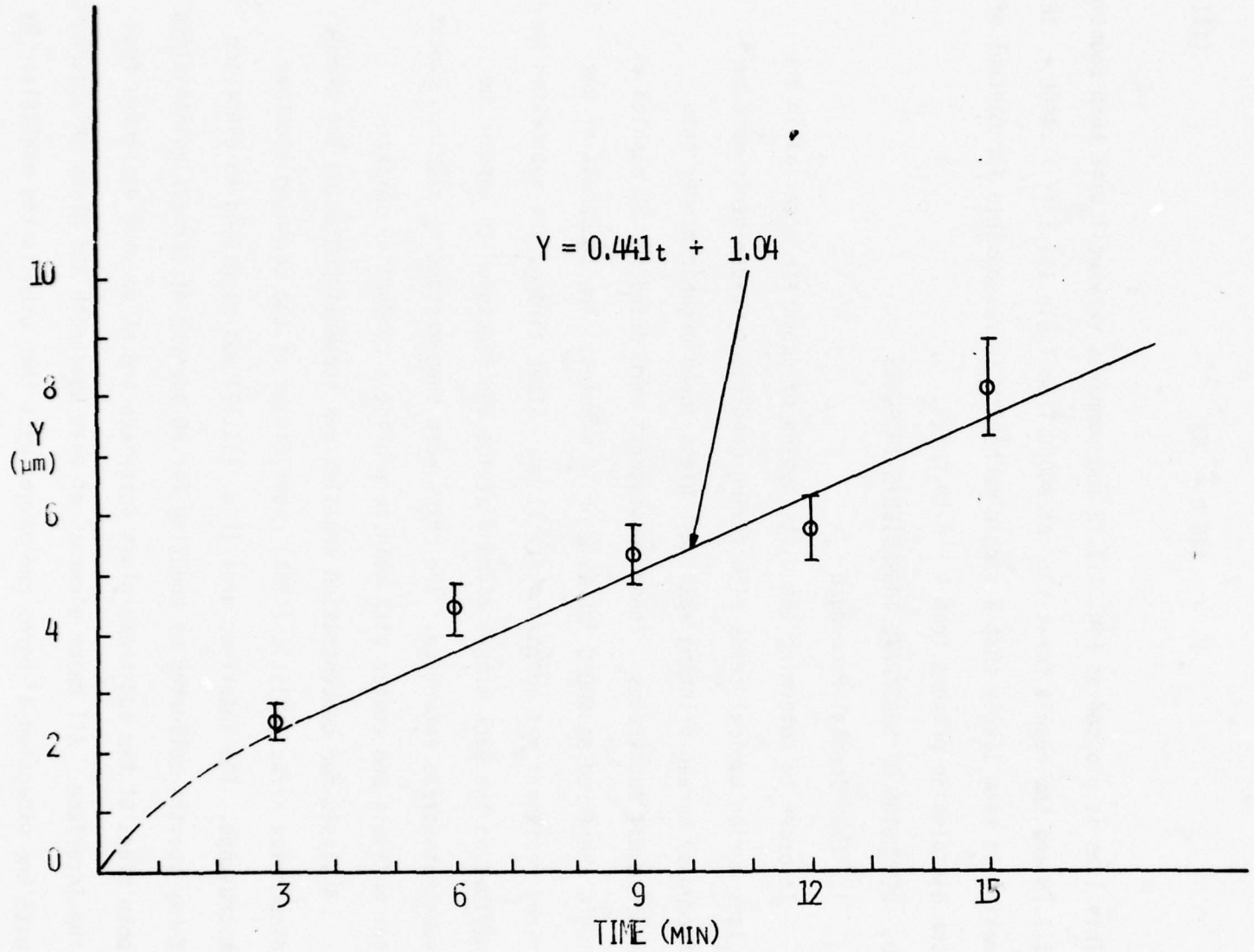

Figure III.11 DISSOLUTION OF ALSi7MG 614 AT 800°C

substrates over the initial segment ($t < t_c$) at 800°C from weight change experiments and making a least squares fit yields

$$Y = .440\ t + .83 \qquad \text{(III.19)}$$

This line is plotted as Fig. III.12 and compares very well with both Equation III.18 and the result for $t < t_c$ at 800°C from Table III.1 ($Y = .440t + .16$) making it seem likely that a single mechanism is responsible for control of the dissolution process from $t = 0$ to $t = t_c$.

D. DIFFUSION OF SUBSTRATE INGREDIENTS IN GLASS

1. Experimental Procedure

In order to determine the distribution of substrate material in the glass during typical thick film firing conditions, experiments were performed by screen printing -325 mesh glass in an organic binder onto AlSiMag 614 substrates. These "resistors" were dried for 30 minutes at 120°C and fired at 800°C for 4, 8 or 10 minutes. The thickness of the fired resistors was approximately 11 μm. After firing, the substrates were scribed on the back with a diamond stylus and fractured to expose the substrate-glass interface. The chips were then mounted on aluminum blocks for analysis and coated with gold to provide a conductive surface.

Analysis for concentration profiles was accomplished using the energy dispersive X-ray analysis (EDAX) capabilities of the scanning electron microscope. The interface area (Fig. III.13) was magnified to 6500X and X-ray spectra collected by counting for 80 seconds at various points along both sides of the substrate-glass interface and at varying distances from the interface. All major elements of both substrate and glass (Al,Si,Pb,Mg) with the exception of boron and oxygen were then used in the analysis. By

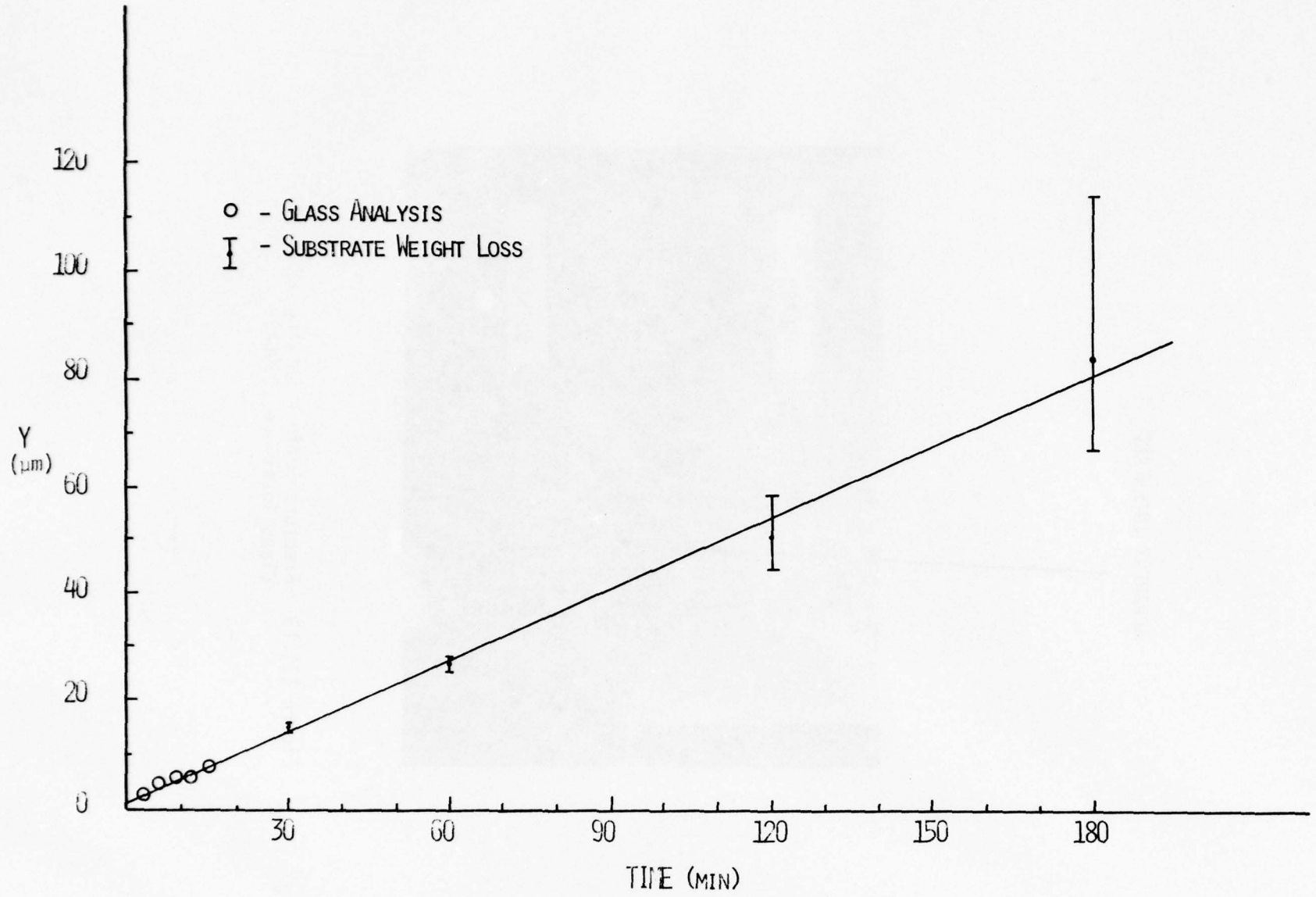

Figure III.12 Dissolution of ALSiMag 614 at 800°C

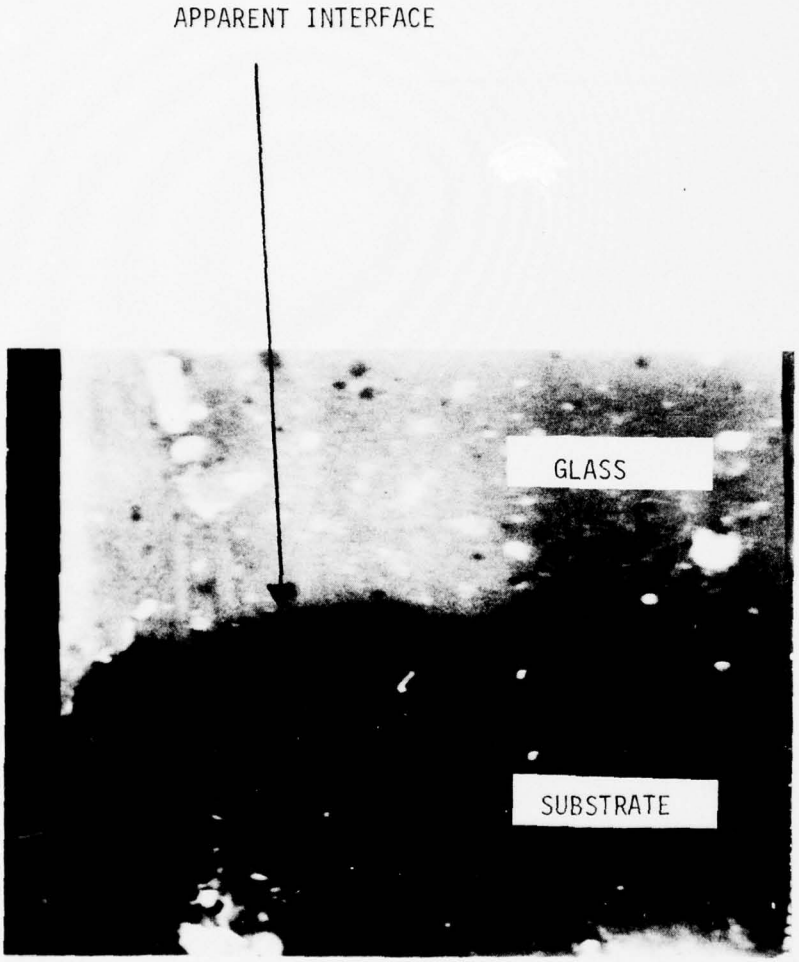

Figure III.13 Fracture Surface Showing Substrate-Glass Interface (6500X)

calling up the appropriate computer program (ZAF), the concentrations of the elements in weight per cent were obtained. These data were then converted to weight per cents of the oxides, and the results for Al_2O_3 and PbO plotted as a function of distance from the interface; the results for SiO_2 and MgO showed similar behavior. An EDAX analysis of model glass which had no substrate contact showed a 2.5 w/o alumina background level, probably due to the aluminum mounting blocks.

2. Results and Analysis

Figures III.14 - III.16 show data obtained with the SEM EDAX representing the substrate-resistor glass diffusion couple. The plotted data have been corrected according to standard calibration procedures [20]. The spot size of the electron beam is quite small, approximately 100 Å, but the source of X-rays is much larger due to multiple scattering of the incident electrons in the material. An X-ray source diameter of 4 - 5μm would be typical for these types of materials, and the apparent gradual change in concentration over a width of about 4 μm could be solely due to the size of the X-ray source in the sample.

The solid lines drawn in Figs. III.14 - III.16 are based on the following assumptions: 1) a step change in concentration at the substrate-resistor interface as shown at the top of the graphs; 2) an X-ray source diameter of 4.8 μm in both substrate and glass; and 3) an X-ray intensity distribution that is conical with a peak value at the apex located at the center of the source and decreasing to zero at 2.4 μm, the assumed radius of the source. The detailed analysis to obtain these curves is presented in Appendix B. Having the X-ray source diameter be the same in both the substrate and the glass was done for methematical convenience. The X-ray source diameter of 4.8 μm was selected for a good fit with the data, but that size is consistent

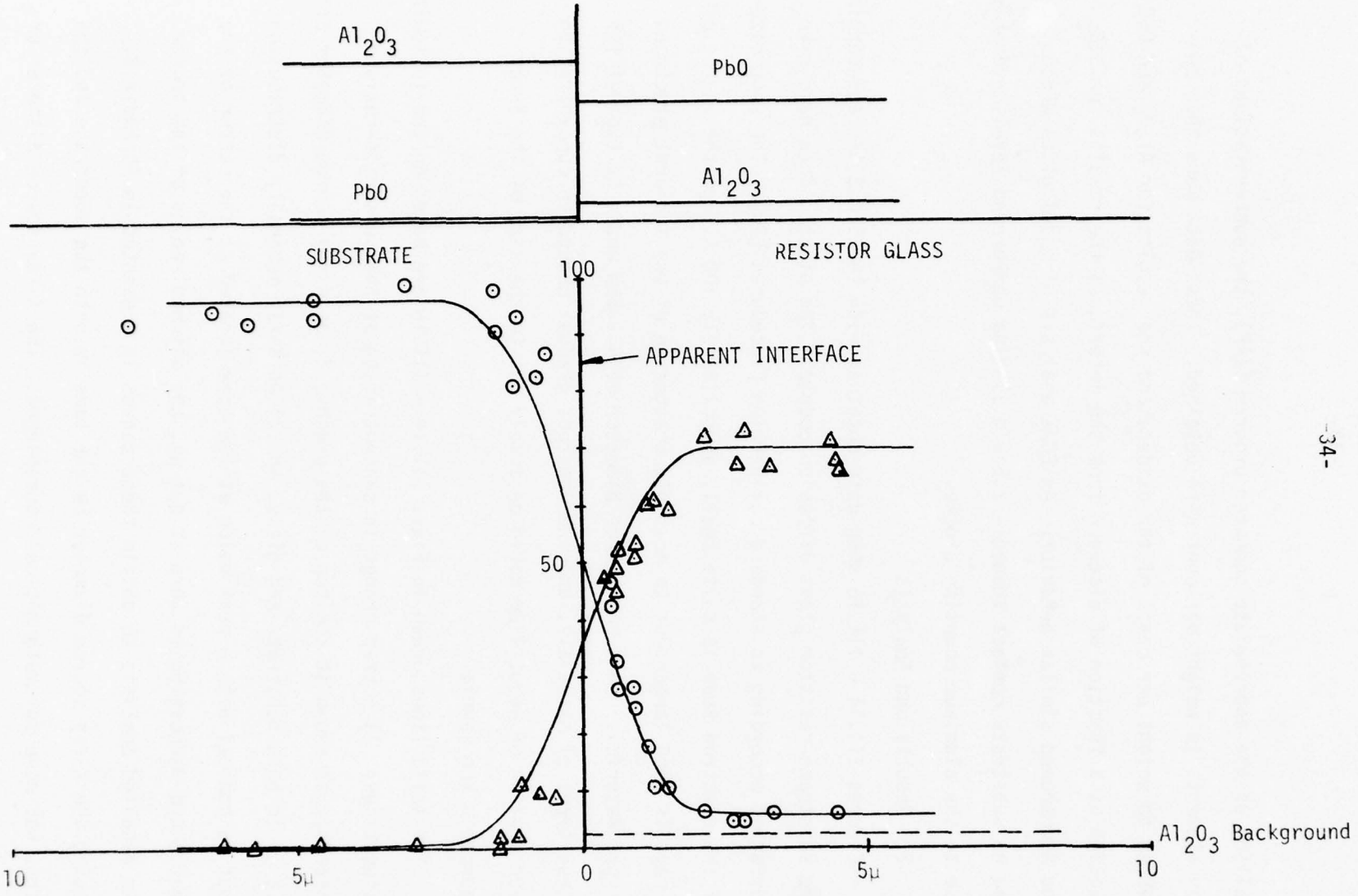

Figure III.14 DIFFUSION ACROSS RESISTOR-SUBSTRATE INTERFACE (800°C, 4 minutes)

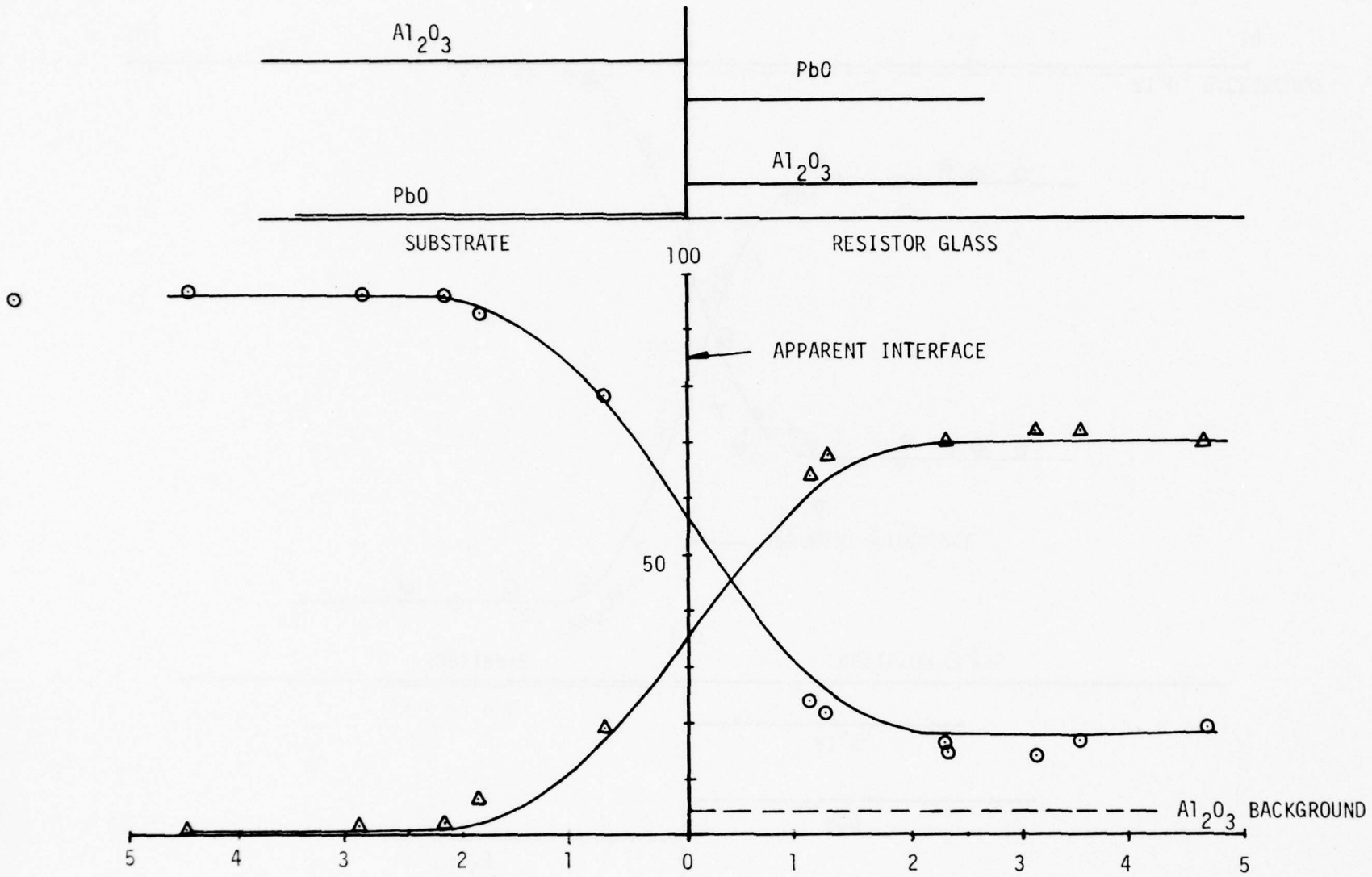

Figure III.15 DIFFUSION ACROSS RESISTOR-SUBSTRATE INTERFACE (800°C, 8 minutes)

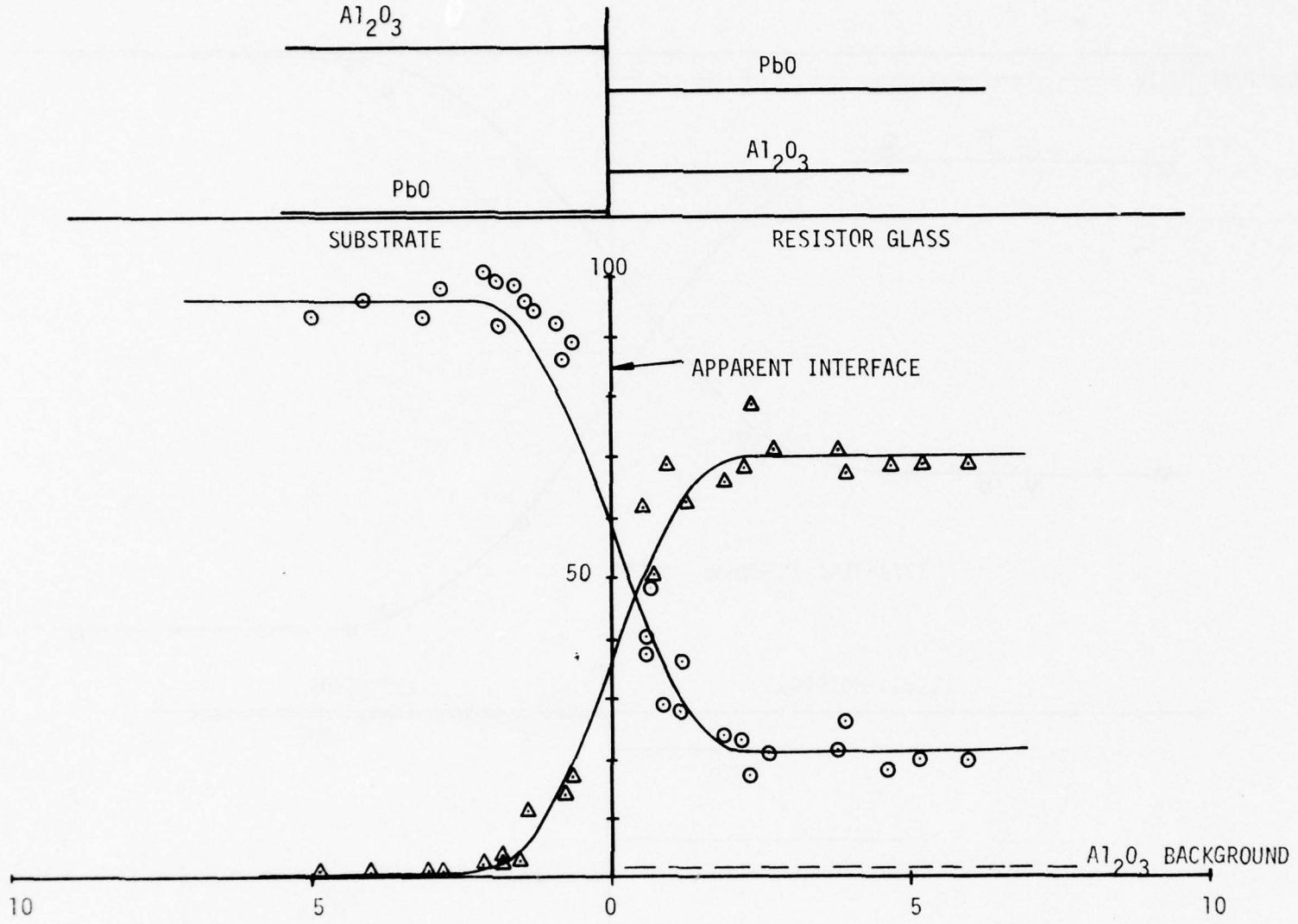

Figure III.16 DIFFUSION ACROSS RESISTOR-SUBSTRATE INTERFACE (800°C, 10 minutes)

with previously measured values in materials of similar average atomic weights [20]. X-ray intensity distributions should be gaussian, ignoring fluorescence, but a conical intensity distribution was chosen for mathematical convenience. The assumed step changes in concentration at the substrate-resistor interface result in a close agreement between the apparent measured concentrations and the calculated values.

E. DISCUSSION

Of the three mechanisms which could limit the dissolution rate of alumina in the presence of glass (see Section III.A) the molecular diffusion model must be discarded immediately because none of the data for substrate recession (Y) as a function of time collected by any of the experimental techniques could be fit to a $t^{\frac{1}{2}}$ dependence as required for this model (see Eq. III.4). The other two mechanisms, phase boundary reaction rate and diffusion through a boundary layer under natural convection, both predict a linear dependence of Y on time, and this was the observed behavior at all times and temperatures with both AlSiMag 614 and AlSiMag 772 substrates. Both substrates showed a change to a smaller but still constant recession rate after some time t_c, but the time-temperature relationships important in thick film processing lie within the first segment, i.e. times less than t_c.

The results from studies of the diffusion of substrate ingredients in the glass are best interpreted in terms of a step function change in concentration at the interface and a constant concentration of substrate ingredients throughout the glass. This means that diffusion of substrate ingredients away from the interface region must be fast in comparison to the movement of atoms across the interface, thereby favoring the reaction rate limiting mechanism. If the initial dissolution is under chemical control, any change in surface area of the substrate will cause a change

in the recession rate according to Eq. III.1. The ratio of actual to geometric area (A_c/A_o) for AlSiMag 614 substrates was found to be 2.42 by the BET technique using Xenon absorption at liquid nitrogen temperatures [21]. This value is consistent with the topology of the virgin substrate surfaces shown in Fig. II.1a. However, when the substrate is in contact with the glass at 800°C, the smaller surface grains are rapidly removed bringing larger,more rounded grains to the substrate-glass interface, as shown in Figs. II.1b - II.1d. Beyond 3 minutes contact time, there is very little difference in appearance between the surfaces up to 12 hours of contact (Fig. II.1d). Figure II.1 indicated that there is a significant decrease in A_c during the first 2 or 3 minutes of firing with very little change thereafter. If this is the case, then the dashed portion of Fig. III.11 is real and is due to this surface area change.

At longer glass-substrate contact times ($t > t_c$) it is possible that the kinetics are controlled by the rate of diffusion through a boundary layer under natural convection, but this cannot be proven without additional data. Since the times involved are much greater than any involved in thick film processing, the rate controlling mechanism in this regime was not explored further.

The differences between the behavior of AlSiMag 614 and AlSiMag 772 substrates can be explained on the basis of differences in composition, microstructure and surface areas. Based on the differences observed in dissolution rate for basal plane and off basal plane sapphire (Fig. III.9) the differences can be explained solely on the basis of preferred orientation with the 772 substrates. At longer times ($t > t_c$) the dissolution rates are the same for the 614 and 772 substrates. If the rate controlling mechanism in this time regime is boundary layer diffusion, microstructure

differences would be totally unimportant and the small difference in composition should have very little effect on the diffusion coefficient.

IV. ELECTRICAL EFFECTS

The objective of this phase of the research is to determine the electrical properties of thick film resistors as a function of the amount of substrate dissolved in the glass. Experiments have examined the temperature coefficient of resistance (TCR), and the current-voltage relationship, which has indicated indirectly the voltage coefficient of resistance (VCR).

A. EXPERIMENTAL PROCEDURE

Since the amount of alumina substrate dissolved in the glass was to be an independent variable, a substrate other than alumina had to be found. Ideally, the substitue would be non-conducting and non-reacting so that RuO_2-glass inks could be screen-printed, fired, and tested as normal thick-film resistors. Until the "ideal" substrate can be found, platinum foil has been used as a non-reacting substrate for firing composites of roughly rectangular shapes (.1cm x.4cm x 1.0cm).

By trial-and-error, it was determined that the solubility limit of AlSiMag 614 substrates in the model glass was approximately 8 w/o. The substrates were cleaned then broken up before adding them to a platinum crucible with an appropriate amount of fritted glass. The glass and substrate pieces were heated to 1000°C, held until the alumina had dissolved, and then the temperature was reduced to 800°C and held in order to make sure no alumina would precipitate out at the maximum firing temperature. The glass solution at 800°C was fritted in deionized water

and ground to -325 mesh in either an agate or an alumina vibratory one ball mill.

All resistor compacts made to date have contained 5 w/o RuO_2 and 95 w/o glass. The powders were weighed, mixed, pressed into cylinders 6 mm in diameter by about 12 mm in length in a uniaxial press, and isostatically pressed at 40 ksi. The compressed cylinders were fired in boats made from 0.06 mm Pt foil; a typical boat was 2mm x 4 mm x 12 mm. Some resistors were fired in a constant temperature box furnace at 800°C for 15 minutes then transferred to a second furnace to be annealed at 450°C for 1 hour. Other resistors were fired in an automatically controlled push-rod furnace which allowed a change in the time-temperature profile by changing a cam. The normal firing profile for the push-rod furnace was: heated at 12.5°C per minute from room temperature to 800°C, held for 15 minutes, cooled to 450°C at 50°C per minute, held for 1 hour, and cooled to room temperature at 25°C per minute.

Four terminal connections were made to the resistors to eliminate contact resistance problems during testing. Platinum wire (.025 mm) was wrapped around the resistor at each end and approximately 5 mm in from each end. A conducting epoxy was then painted over the wire and the composite and cured at 200°C overnight.

The temperature coefficient of resistance (TCR) of these devices was measured by monitoring the resistance as a function of temperature. The temperature was controlled by an environmental chamber and varied from -55°C to +125°C. The potential drop across the voltage contacts was measured directly while the current was calculated from the measured voltage across a precision resistor in series with the current leads. The same basic circuit was used for the current-voltage measurements, only the temperature was kept constant at 23°C.

B. RESULTS AND ANALYSIS

The TCR experiments have shown a substantial difference between RuO_2-glass composites with and without substrate present. Figure IV.1 shows normalized resistance as a function of temperature for devices fired by two different methods. Type 1 resistors were fired in the constant temperature furnace, and Type 2 composites were fired in the push-rod furnace as described in Section IV A above.

Those samples without dissolved substrate in the glass showed very similar characteristics over the entire temperature range tested. The hot TCR was +400 ppm/°C and the cold TCR was +360 ppm/°C. Composites with 8 w/o substrate dissolved in the glass, in contrast to those mentioned above, showed a very low TCR. The hot TCR for Type 1 was +28 ppm/°C and for Type 2 was +110 ppm/°C, while the cold TCR for Type 1 was -10 ppm/°C and for Type 2 was + 25 ppm/°C. Subsequent experiments on new samples have re-enforced these results.

The current density-electric field behavior for thick film resistors made from RuO_2 and the model glass has been shown to be linear over several orders of magnitude [3]. RuO_2-glass composites used in this study were all composed of 5 wt % RuO_2 relative to glass, which corresponds to 3.3 vol.%. From the previously determined [3] blending curve this corresponds to a sheet resistance of 1.07×10^5 ohms per square-mil , or a resistivity of 270 ohm-cm. The current density-electric field behavior that is known to apply to these resistors is shown as the calculated line on Fig. III.2 along with data from a composite made with the model glass and one made with the model glass containing 8 wt% dissolved substrate. The composite made with glass containing no substrate shows linear behavior similar to thick film resistors made with this glass, but the resistivity is lower by an order of magnitude. In contrast, the

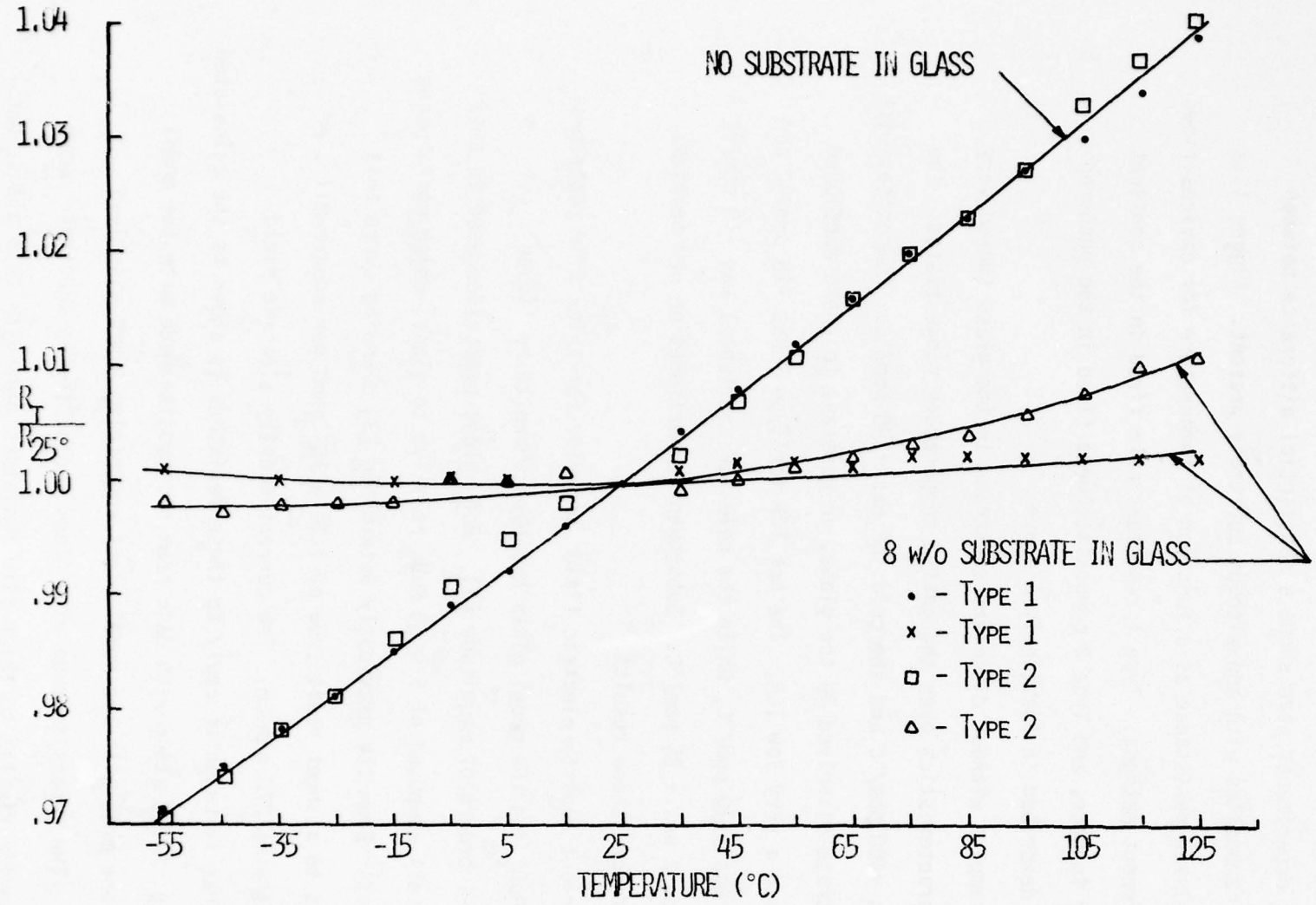

Figure IV.1 NORMALIZED RESISTANCE VERSUS TEMPERATURE FOR RuO_2-GLASS COMPOSITES

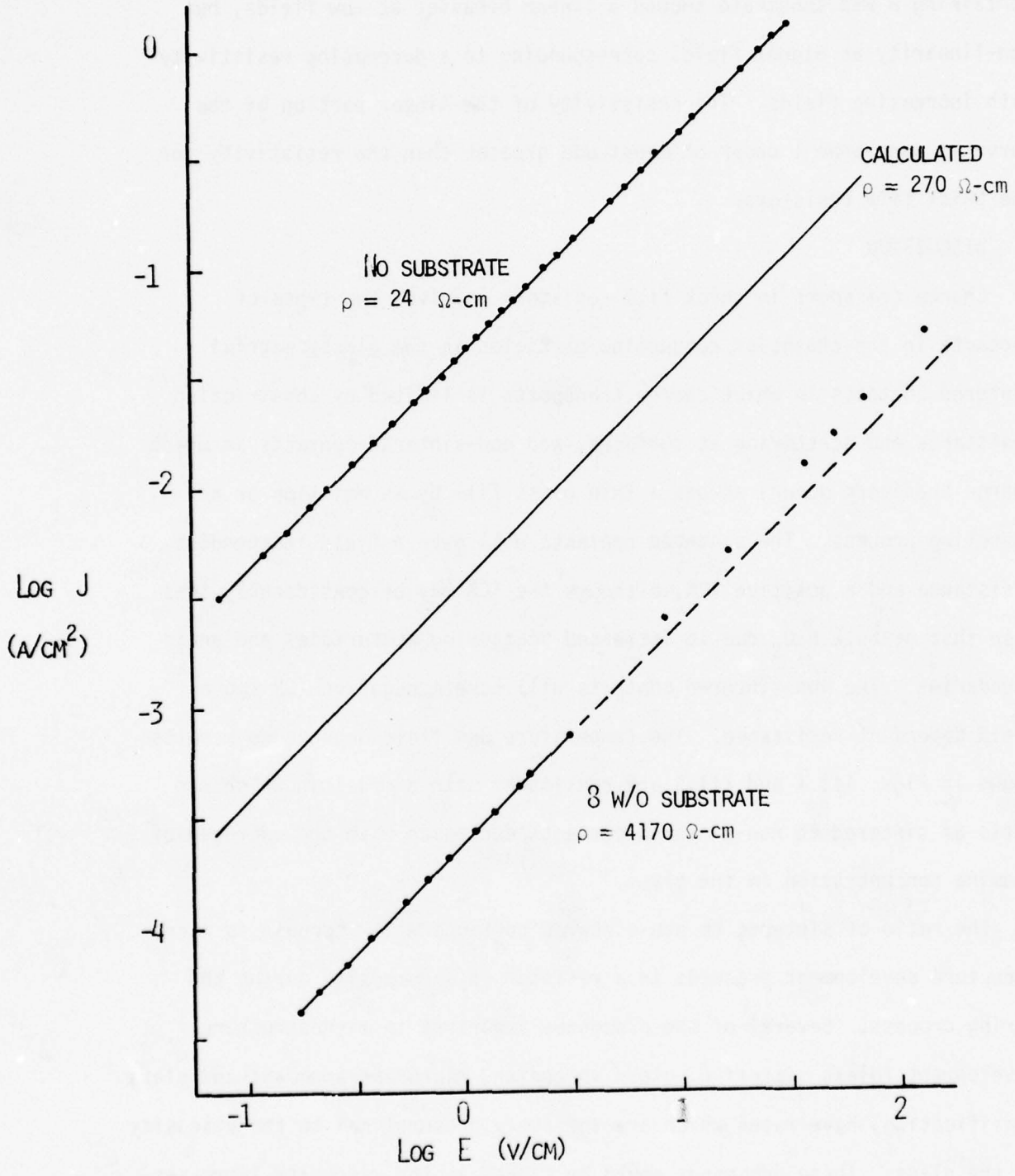

Figure IV.2 CURRENT DENSITY - FIELD RELATIONSHIPS FOR RuO_2-GLASS COMPOSITES

current density-electric field behavior of the composite made with glass containing 8 wt% substrate showed a linear behavior at low fields, but non-linearity at higher fields corresponding to a decreasing resistivity with increasing fields. The resistivity of the linear portion of the curve is more than 1 order of magnitude greater than the resistivity for the thick film resistors.

C. DISCUSSION

Charge transport in thick film resistors involves two types of contacts in the chains of conducting particles in the glassy matrix: sintered contacts in which charge transports is limited by constriction resistance and scattering at surfaces, and non-sintered contacts in which charge transport occurs across a thin glass film by an emission or a tunneling process. The sintered contacts will have a field independent resistance and a positive TCR, although the TCR may be considerably less than that of bulk RuO_2 due to increased scattering at surfaces and grain boundaries. The non-sintered contacts will have a negative TCR and a field dependent resistance. The temperature and field dependence results shown in Figs. III.1 and III.2 are consistent with a model in which the ratio of sintered to non-sintered contacts decreases with the increase of alumina concentration in the glass.

The ratio of sintered to non-sintered contacts will increase as microstructure development proceeds in a resistor or a composite during the firing process. Several of the processes important in microstructure development (glass sintering, glass spreading, microrearrangement and glass densification) have rates which are inversely proportional to the viscosity of the glass. These processes would be slowed as the viscosity increases with increasing alumina content, accounting for the increased resistance

and more negative TCR for the composites containing alumina in the glass. The resistivity for the thick film resistors is intermediate between the two composite cases because the glass begins with no dissolved alumina, but has an alumina content that increases with time during the firing. The processes which occur early in the firing sequence (glass sintering, glass spreading and microrearrangement) would have kinetics similar to those in the composites containing glass with no dissolved substrate, but the glass densification process, which occurs late in the firing sequence, would have kinetics more similar to the composite containing 8 wt% substrate dissolved in the glass. Therefore, the calculated line of Fig. IV.2 should lie between the two composite lines as observed.

V. FUTURE WORK

Studies of the kinetics of dissolution and the diffusion of the dissolved species of AlSiMag 614 and AlSiMag 772 substrates will be studied utilizing a commercial glass having a considerably higher viscosity than the model glass. Experimental techniques will be identical to those discussed in this report, but the range of times and temperatures will not be as extensive. The qualitative effects of glass composition on the kinetics of bubble motion and the development of macronetworks of conducting particles in thick film resistors will be determined utilizing hot stage microscopy. The effect of glass composition on its viscosity and surface tension will be determined by measuring the kinetics of the sintering of glass spheres as a function of the concentration of the substrate ingredients dissolved in the glass, and the surface tension/viscosity ratio derived from these measurements. The kinetics of Ostwald ripening of RuO_2 in the glass will

be measured by X-ray diffraction line broadening and surface area techniques as a function of glass composition, and the kinetics for the initial stage of liquid phase sintering of RuO_2 will be calculated from these data.

The effect of substrate constituents dissolved in resistor glass on the temperature coefficient of resistance, the voltage coefficient of resistance, short time overload and current noise will be determined. Charge transport across emission contacts and across tunneling contacts in the conductive chains of thick film resistors will be studied as a function of glass composition.

The results from the studies of microstructure development and charge transport as a function of glass composition will be correlated with previously determined models for these processes and specifications for chemical compositions of substrates and glass which will minimize detrimental changes during processing will be developed.

VI. REFERENCES

1. L. Hailes and W. A. Crossland, "Thick Films: Substrate-Conductor Relationship," Electronic Pack. and Prod. (Int), 3-7, July, 1972.

2. W. A. Crossland and L. Hailes, "Thick Film Conductor Adhesion", S. State Tech., 14, 42-47 (1971).

3. R. W. Vest, "Conduction Mechanisms in Thick Film Microcircuits," Final Technical Report, Purdue Research Foundation Grant Nos. DAHC - 15-70-G7 and DAHC -15-73-G8, ARPA Order No. 1642, December 1975.

4. W. M. Faber, Sr., et. al., "Electrical Resistance Element," U.S. Patent No. 3,304,199, Feb. 14, 1967.

5. A. Prabhu, G. L. Fuller, R. L. Reed and R. W. Vest, "Viscosity and Surface Tension of a Molten Lead Borosilicate Glass, J. Amer. Ceram. Soc., 58, 144-145 (1975).

6. A. Prabhu and R. W. Vest, "Investigation of Microstructure Development in RuO_2-Lead Borosilicate Glass Thick Films," Mat. Sci. Res., 10, 399-408 (1975).

7. R. F. Geller and E. N. Bunting, "The System $PbO-B_2O_3-SiO_2$", J. Res. Natl. Bur. Std., 23, 275-283 (1939).

8. D. W. Johnson and F. A. Hummel, "Phase Equilibria and Liquid Immiscibility in the System $PbO-B_2O_3-SiO_2$", J. Amer. Ceram. Soc., 51, 196-201 (1968).

9. R. L. Reed and L. R. Barrett, "The Slagging of Refractories; II. The Kinetics of Corrosion," Trans. Brit. Ceram. Soc., 63, 509-534 (1964).

10. A. R. Cooper, Jr., "Effects of Moving Boundary on Molecular Diffusion Controlled Dissolution or Growth Kinetics," Trans. Faraday Soc. 58, 2468-72 (1962).

11. A. R. Cooper, Jr., and W. D. Kingery, "Dissolution in Ceramic Systems: I, Molecular Diffusion, Natural Convection, and Forced Convection Studies of Sapphire Dissolution in Calcium Aluminum Silicate," J. Amer. Ceram. Soc., 47, 37-43 (1964).

12. R. L. Reed and L. R. Barrett, "The Slagging of Refractories; Part I The Controlling Mechanism in Refractory Corrosion," Trans. Brit. Ceram. Soc., 63, 671-676 (1964).

13. N. McCallum and L. R. Barrett, "Some Aspects of the Corrosion of Refractories," Trans. Brit. Ceram. Soc., 51, 523-548 (1952).

14. B. N. Samaddar, W. D. Kingery, and A. R. Cooper, Jr., "Dissolution in Ceramic Systems: II, Dissolution of Alumina, Mullite, Anorthite, and Silica in Calcium Aluminum Silicate Slag," J. Amer. Ceram. Soc., 47, 249-254 (1964).

15. A. N. Ryabov, T. I. Kiseleva, and L. B. Kulikova, "Rate of Dissolution of Aluminum Oxide in Molten Potassium Bisulfate," ZH Prik Khim, 48, 407-48 (1975).

16. M. Truhlarova, "Dissolution of SiO_2 and Al_2O_3 in Four Basic Glass Melts at Viscosity log η = 2.5," Silikaty, 18, 31-43,(1974)

17. M. Safdar, G. H. Frischat, and H. W. Hermicke, "Korrosion von Aluminumoxid durch Vanadiumpentoxid Schmelyen," Ber. Dt. Keram. Ges., 51, 291-294 (1974).

18. Y. Nakoda and T. L. Schock, "Surface Texture Formation in Al_2O_3 Substrate," J. Amer. Ceram. Soc., 58, 409-412 (1975).

19. J. S. Murday and P. F. Becher, "Thick Film Fracture Mechanics," in NAVAIR Research Program Review, Electronics, 151-163, Feb. 1976.

20. J. I. Goldstein, H. Yakowitz, P. E. Newbury, E. Lifshin, J. W. Colby, and J. R. Coleman, Practical Scanning Electron Microscopy, Plenum Press (1975).

21. M. V. Coleman and G. E. Gurnett, "Surface Area, Structure and Composition of Debased Alumina Substrates," Proc. IERE Conf. No. 31, Loughborough, 1-16, (1975).

APPENDIX A

GLASS ANALYSIS

A procedure for the chemical analysis of thick film glasses for major constituents (PbO, B_2O_3, SiO_2, and Al_2O_3) was developed. The technique is schematically represented by a flow-sheet in Fig. A1. A complete description of each step in the determination is outlined, and additional details can be obtained from standard analytical chemistry texts*. The confidence limit of the procedure, obtained by analyzing standard chemicals corresponding to various major constituents of the glass, is also presented in Table A1.

*
N. H. Furman, Editor, Scotts Standard Methods of Chemical Analysis, Vol. 1 and 2, Fifth Edition, D. Van Nostrand Co., Inc. New York (1939).

I. M. Kolthoff and E. B. Sandell, Textbook of Quantitative Inorganic Analysis, The Macmillan Company. New York (1946).

A. I. Vogel, A Textbook of Quantitative Inorganic Analysis, Including Elementary Instrumental Analysis, Third Edition, Wiley, New York (1961).

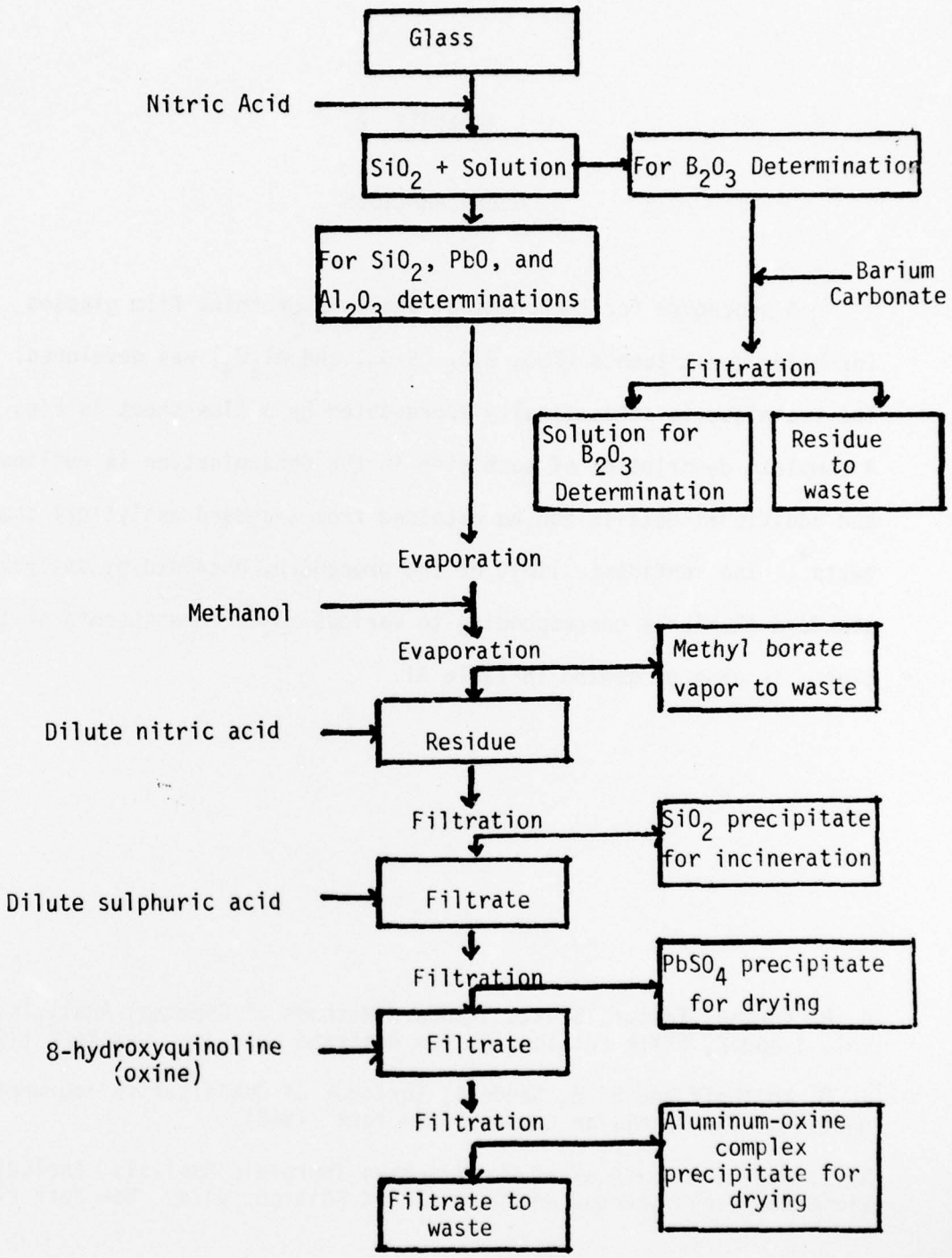

Figure A1. Flow-Sheet for the Separation and the Determinations of PbO, B_2O_3, SiO_2, and Al_2O_3 in Glass.

DETERMINATION OF SiO_2

Principle The acid decomposition of the glass liberates the weak silicic acid ($SiO_2 \cdot XH_2O$). In presence of strong acids such as nitric acid the silicic acid is coagulated. If the solution is evaporated to dryness, the (hydrated) silica loses a considerable amount of moisture, and is rendered insoluble. Evaporation with methanol removes boron as methyl borate. If the residue is taken up with dilute nitric acid, the lead and the aluminum nitrates dissolve, and the insoluble silica can be filtered off.

Procedure About 1 gram of the finely powdered glass sample is weighed into a platinum crucible. The sample is mixed with 1 gram of ammonium nitrate, and 10 ml of 20% nitric acid is added. The contents are heated gently on a water bath until the glass is completely decomposed. Heating is continued until all the acid is evaporated. Then 20 ml of anhydrous methanol is added and the contents of the crucible again evaporated to dryness. Anhydrous methanol readily removes boron as volatile methyl borate. The methanol evaporation is repeated once more. The residue is baked on a sand bath at 120°C for 1 hour to partially dehydrate the silica and render it as insoluble as possible. The residue is taken up with hot dilute nitric acid and filtered immediately using Whatmann #42 filter paper. Gentle suction could be applied to hasten the filtration. The precipitate is washed with 5% nitric acid until free from lead and aluminum. The filtrate is collected in an evaporating dish, the contents evaporated to dryness, and the residue baked at 120°C for 1 hour. The residue is then taken up with dilute nitric acid and

filtered immediately on a fresh filter paper. The residue is washed with 5% nitric acid. combined with the first one, and ignited to constant weight at 1050°C in a previously ignited platinum crucible. The filtrate is saved for PbO and Al_2O_3 determination.

The ignited residue may contain impurity oxides. The amount of impurity can be determined by treating the weighed residue in the platinum crucible with an excess of hydrofluoric acid and 2 ml of concentrated sulphuric acid. The contents of the crucible are evaporated on a gentle flame and then ignited at 1050°C to constant weight. The silica is expelled as the volatile silicon tetrafluoride. The loss in weight represents the amount of pure silica present.

DETERMINATION OF PbO AS $PbSO_4$

Principle Lead sulfate has very little solubility in water (about 0.004 gram per 100 ml. of cold water) whereas aluminum sulfate is very soluble in water. The large difference in solubility is utilized in separating lead and aluminum.

Reaction $PbNO_3 + H_2SO_4 = PbSO_4 \downarrow + HNO_3$

Procedure The filtrate from the SiO_2 determination is reduced to 20 ml in volume. About 5 ml of concentrated sulfuric acid is added, and the mixture is heated on a water bath and then gently on a wire gauze until thick white fumes of sulfuric acid are freely evolved. This ensures the conversion of lead nitrate into lead sulfate and the complete removal of nitric acid. The contents are cooled, diluted carefully with 50 ml of water, and allowed to stand for 2 hours. The lead sulfate precipitate is filtered off through a Gooch filtering crucible. The precipitate is washed with 1% sulfuric acid and then with the minimum quantity of cold water saturated with lead sulfate. The filtrate is

saved for Al_2O_3 determination. The precipitate is dried at 130°C to constant weight.

$$PbO \equiv 0.7359\ PbSO_4$$

DETERMINATION OF Al_2O_3 USING 8-HYDROXYQUINOLINE

Principle The compound 8-hydroxyquinoline (oxine or quinolinol), HC_9H_6NO, forms compounds with metals, the metal ion replacing the hydrogen atom. Most of the common metals, with the exception of alkali metals, form complexes with oxine if the pH is appropriate. Aluminum can be precipitated in a slightly acidic solution. Because lead also is precipitated in acidic solution, it should be removed prior to Al_2O_3 determination. Magnesium and calcium are not precipitated in acidic medium.

Reaction $Al_2(SO_4)_3 + 6\ HC_9H_6NO = 2\ Al(C_9H_6NO)_3 \downarrow + 3H_2SO_4$

Procedure The filtrate from PbO determination is neutralized by adding solid sodium carbonate in small quantities at a time. Then 1 ml of dilute sulfuric acid is added to make the solution slightly acidic. The solution should not contain more than the equivalent of 0.05 gram of aluminum for every 100 ml of the solution. The solution is warmed up to 80°C, and a slight excess of 5% solution of 8-hydroxiquinoline in 2N acetic acid is added, allowing 1 ml of the reagent for each 3 milligrams of aluminum present. Then 2N ammonium acetate is slowly added with constant stirring until a permanent precipitate forms, and then 25 ml more of the acetate added to ensure complete precipitation. The contents are allowed to stand at room temperature for 2 hours, and the precipitate is collected in a Gooch filtering glass crucible. The precipitate is washed with cold water and dried at 130°C to constant weight.

$$Al_2O_3 \equiv 0.1111\ Al(C_9H_6NO)_3$$

DETERMINATION OF B_2O_3 BY $BaCO_3$ METHOD

Principle Boric acid acts as a weak monobasic acid in water. However, in the presence of certain polyhydroxy compounds such as mannitol, glucose, or glycerol, it acts as a much stronger acid and can be titrated to a phenolphthalein end point. The $BaCO_3$ method is based on the fact that barium borate, formed by the addition of barium carbonate to boric acid, is quite soluble, and that the barium carbonate buffers the solution to such a pH as to cause the precipitation of the hydroxides of lead and aluminum. Insoluble barium compounds of silica are also formed.

Reaction H [boric acid complex] + NaOH = Na [Boric acid complex] + H_2O

Procedure About 1 gram of the finely powdered glass sample is weighed into a platinum crucible. The sample is mixed with 1 gram of ammonium nitrate, and 10 ml of 20% nitric acid is added. The contents are heated gently on a water bath until the glass is completely decomposed, taking care not to boil because boron has a tendency to escape with moisture. The free acid is nearly neutralized by adding sodium carbonate in small quantities, but care should be taken to see that the solution is slightly acidic before barium carbonate is added. The solution is diluted with 50 ml of water and transferred to a distillation flask. About 5 grams of barium carbonate is added and the contents boiled under a reflux condenser for at least five minutes. The volume of the solution should be at least 50 ml for every 0.25 gram of B_2O_3 present in order to avoid precipitation of B_2O_3 as barium borate. The contents of the flask are allowed to stand for 2 hours. The residue is filtered off and washed with water. The filtrate is acidified with HCl and boiled in a

distillation flask under a reflux condenser to remove CO_2. The filtrate is then neutralized with NaOH using methyl orange or methyl red indicator. The solution is made up in a 100 ml standard measuring flask, 30 ml of the solution pipetted out into a conical flask, about 1 gram of mannite added, and the contents titrated with 0.1N sodium hydroxide using phenolphthalein indicator. The end point is the first appearance of a permanent pink color unaffected by the addition of mannite. The titration is repeated for concordant titer values.

1 ml of 1N NaOH $\equiv$ 0.03483 gram of B_2O_3

TABLE A1. RESULTS OF ANALYSIS OF STANDARD CHEMICALS

Species Analyzed	Amount in Grams		% Error	Remarks
	Taken	By Analysis		
Pb_3O_4	1.1666	1.1729	0.5	Pb_3O_4 was fused with H_3BO_3, SiO_2, Al_2O_3, and Na_2CO_3 before analyzing
H_3BO_3	0.2660	0.2673	0.5	H_3BO_3 was mixed with Pb_3O_4 and $Al(NO_3)_3$ before analyzing
SiO_2	0.1200	0.1170	2.5	SiO_2 was fused with Pb_3O_4, H_3BO_3, Al_2O_3, and Na_2CO_3
Al	0.0856	0.0854	0.3	Al powder was mixed with Pb_3O_4 and H_3BO_3

APPENDIX B

ANALYSIS OF EDAX RESULTS

Although the SEM electron spot size is of the order of 100 Å in diameter, the incident beam electrons scatter repeatedly in the sample and create an X-ray source size of diameter 1 - 5 μm. The concentration of X-ray intensity is gaussian in cross section, and the exact size depends upon the incident energy and density of the sample. The total source of X-rays is the volume integral under the three dimensional concentration profile graph. However, this integration does not lead to calculatable formulas for the case when the X-ray source crosses an interface boundary. Therefore, in order to work with an easier integral, the concentration profile of the X-ray source is assumed to be conical as represented in the figures below.

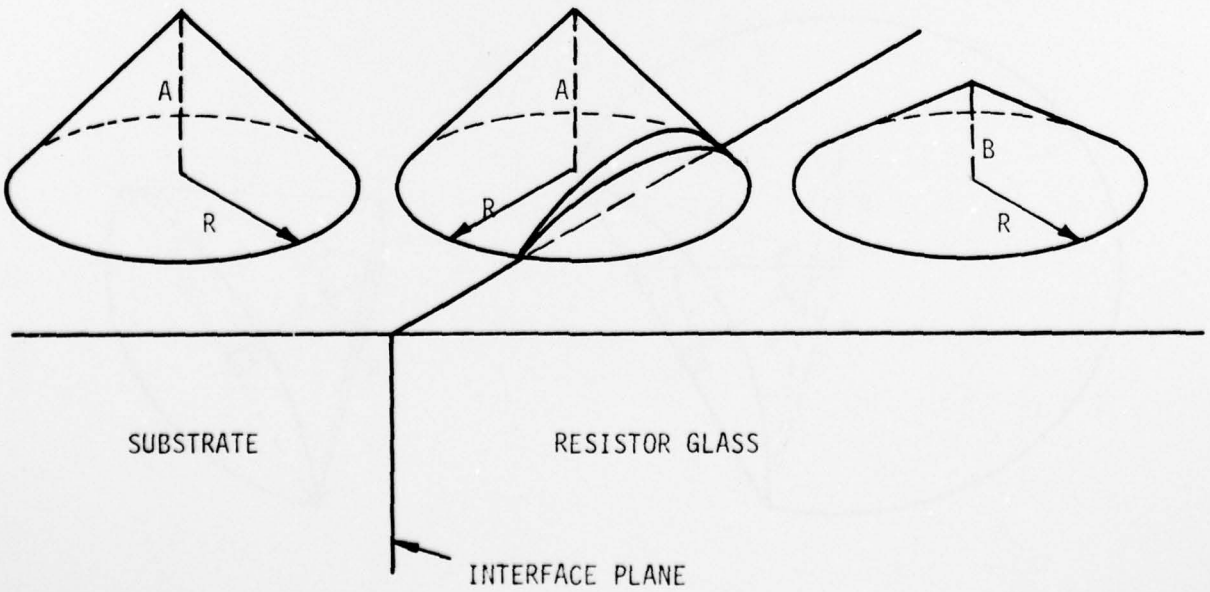

The case shown is for Al_2O_3, detected by the X-ray intensity of aluminum atoms. Therefore, on the substrate side the height of the concentration cone is A whereas the height on the resistor glass side is B, a much lower value. It has been assumed for mathematical convenience that the diameter of the source, 2R, is the same in both materials.

The center view represents the X-ray source crossing the interface. The fraction of the source intensity coming from the substrate is represented by a sectioned cone of height A, and the fraction of the source intensity coming from the glass is represented by a section of height B. The sum of the two partial volumes is taken to be proportional to the X-ray intensity.

The figure below shows the volume portion that requires integration. A segment of the cone has been removed a distance X from the center of the cone and it subtends an angle 2 θ_o.

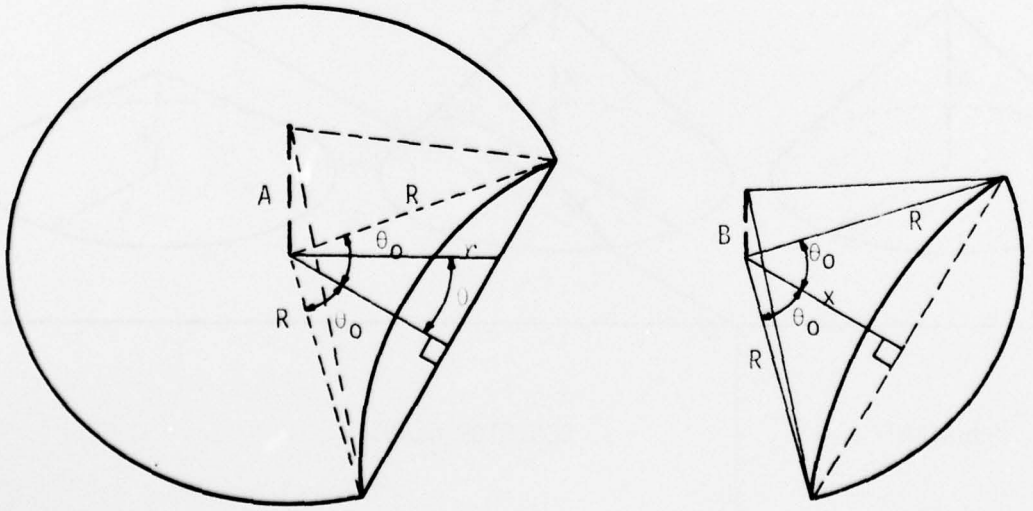

The volume of this portion is

$$V_i = \int_{-\theta_o}^{+\theta_o} \int_{r=o}^{r=\frac{x}{\cos\theta}} \frac{A}{R} (R - r)\, r\,dr\,d\theta$$

$$= \frac{A}{2} \int_{-\theta_o}^{+\theta_o} \left(\frac{x}{\cos\theta}\right)^2 d\theta - \frac{A}{3R} \int_{-\theta_o}^{+\theta_o} \left(\frac{x}{\cos\theta}\right)^3 d\theta$$

$$= Ax^2 \tan\theta_o - \frac{Ax^3}{3R}\left[\frac{\sin\theta_o}{\cos^2\theta_o} + \frac{1}{2} \ln\left(\frac{1+\sin\theta_o}{1-\sin\theta_o}\right)\right]$$

The volume of the remaining portions is the angle fraction of the volume of a cone.

$$V_2 = \frac{AR^2}{3} (\pi - \theta_o)$$

The total volume of the figure shown is $V_a = V_1 + V_2$. Similarly, the volume of the cone segment of height B is

$$V_B = \frac{BR^2}{3}\theta_o - Bx^2\tan\theta_o + \frac{Bx^3}{3R}\left[\frac{\sin\theta_o}{\cos^2\theta_o} + \frac{1}{2} \ln\left(\frac{1+\sin\theta_o}{1-\sin\theta_o}\right)\right]$$

When the X-ray source is predominantly in the resistor glass the volume terms are the same except that the values of A and B are interchanged.

The heights of the cones, A and B, are chosen to be values such that the weight percents of Al_2O_3 and PbO are the correct values on both sides of the interface (96% and 70% respectively). The measured X-ray intensity is usually not a direct measure of the concentration of

material in the sample. The data must be calibrated by a standard and then corrected for fluorescence and absorption.* For this particular sample, these corrections for Al_2O_3 in the substrate and PbO in the glass are trivial since their concentrations are known. The concentration of PbO in the substrate is essentially zero and does not need to be corrected. The X-ray intensity of Al_2O_3 in the glass has been corrected with the same factor used on the substrate side. This ignores differences in absorption and fluorescence on both sides but the error is not considered significant.

*J. I. Goldstein, H. Yakowitz, P. E. Newbury, E. Lifshin, J. W. Colby, and J. R. Coleman, Practical Scanning Electron Microscopy, Plenum Press (1975).

DISTRIBUTION LIST

Naval Air Systems Command
Washington, D.C. 20361
Attn: AIR-310B (15)

Naval Air Systems Command
Washington, D. C. 20361
Attn: AIR-360

Naval Air Systems Command
Washington, D. C. 20361
Attn: AIR-52022F

Naval Air Systems Command
Washington, D. C. 20361
Attn: AIR-954 (14)

E. I. duPont Nemours
Electrochemical Department
Experimental Station
Bldg. 173
Wilmington, Delaware 19898

Director
Naval Research Laboratory
Washington, D. C. 20390
Attn: Dr. J. Murday (2)

Commander
Naval Avionics Facility
21st & Arlington Avenue
Indianapolis, Indiana 42618
Attn: Mr. D. Tague

Commander Naval Avionics Facility
21st & Arlington Avenue
Indianapolis, Indiana 42618
Attn: Mr. M. Cowart

Advisory Group on Electron Dev
201 Varick Street
New York, New York 10014
Attn: Secretariat on LP Devices

Plessey, Inc
20245 Sunburst Street
Chatsworth, CA 91311
Attn: Mr. E. Rodgers

Westinghouse D&E Systems Center
P.O. Box 1897, M.S. 717
Barltimore, MD 21203
Attn: Dr. Ted Foster

Monsanto Research Corporation
Dayton Laboratory
1515 Nicholas Road
Dayton, Ohio 45477
Attn: Dr. R. Janowiecki

Director, ARPA
1400 Wilson Blvd
Arlington, Virginia 22209
Attn: Dr. A. Bement

National Bureau of Standards
Bldg 225, Rm A-331
Washington, D. C. 20234
Attn: Mr. G. Harmon

Commander
Naval Electronics Laboratory Center
San Diego, CA 92152
Attn: Mr. O. Lindberg, Code 4800

Commander
Naval Weapons Center
China Lake, CA 93555
Attn: Dr. F. Essig, Code 601

Mr. Jack Ferrel
RADC/RBRM
Griffiss AFB, New York 13440

RCA
David Sarnoff Research Center
Princeton, New Jersey 08540
Attn: Dr. T. Hitch (2)

Western Electric Engr Research Ctr
Box 900
Princeton, New Jersey 08540
Attn: Dr. D. J. Shanefield

Western Electric Engr Research Ctr
Box 900
Princeton, New Jersey 08540
Attn: Dr. J. R. Piazza

Bell Laboratories
Allentown, PA 18103
Attn: Dr. H. Cohen

Bell Laboratories
Allentown, PA 18103
Attn: Dr. Y. Kim

Commanding Officer
AMSEL-TLIT
Fort Monmouth, New Jersey 07703
Attn: H. C. Frenkel

Hybrid Microcircuit Technology
Div. 2431
Sandia Laboratories
Albuquerque, NM 87115
Attn: Dr. R. K. Traeger (Div 2431)

Hybrid Microcircuit Technology
Div 2431
Sandia Laboratories
Albuquerque, NM 87115
Attn: Dr. J. T. Grissom (Div 2432)

Materials Research Laboratory
Department of Ceramic Science
Pennsylvania State University
University Park, PA 16302
Attn: Prof. J. V. Biggers

Reliability Analysis Center
Griffiss AFB, NY 13441
Attn: I. L. Krulac

State of the Art, Inc.
1315 South Allen
State College, PA 16801
attn: Mr. D. Hamer

Thick Film Systems, Inc.
324 Palm Avenue
Santa Barbara, CA 93101
Attn: Mr. J. Provance

Rockwell International
Autonetics Division
Anaheim, CA 92803
Attn: J. Licari-Microcircuits

Commanding General
U. S. Army Electronics Command
Green Acres Bldg.
Ft. Monmouth, NJ 07703
Attn: J. Kelly-AMSEL-PP-1P1-1